Organoplatinum-Bridged Cyclotribenzylene Dimers

Jing Zhang, Frédéric Aribot, Jean-claude Chambron, Nathalie Zorn, Emmanuelle Leize-wagner, Marion Jean, Nicolas Vanthuyne, Enrique Espinosa, Emmanuel Aubert

EurJIC
European Journal of Inorganic Chemistry

Research Article
doi.org/10.1002/ejic.202300284

Chemistry Europe
European Chemical Societies Publishing

www.eurjic.org

Organoplatinum-Bridged Cyclotribenzylene Dimers

Jing Zhang,[a] Frédéric Aribot,[a] Jean-Claude Chambron,*[a] Nathalie Zorn,[b] Emmanuelle Leize-Wagner,*[b] Marion Jean,[c] Nicolas Vanthuyne,*[c] Enrique Espinosa,[d] and Emmanuel Aubert*[d]

Cyclotribenzylenes (CTBs) combining carbonitrile (−CN) and alkyne (−C_2H) substituents were synthesized as racemic mixtures and resolved by HPLC on chiral stationary phases. Two of these compounds were used to prepare platinum-bridged CTB dimers, in which Pt^{II} is bound to the CTBs via Pt–alkynyl bonds in *cis* configuration. The organometallic complexes were examined by mass spectrometry and NMR spectroscopy, which indicated that they were obtained as mixtures of diastereoisomers (a *meso* or *syn* form and a pair of chiral or *anti* forms) when racemic CTBs were used. Enantiomerically pure complexes were prepared from resolved CTBs, which allowed us to distinguish the NMR signals of the chiral and *meso* forms in the diastereoisomeric mixtures. In certain conditions, the platinum complexes played the role of a pincer π-alkynyl ligand for Cu(I) coming from the copper iodide used as a synthetic auxiliary. The Cu^+ cations could be easily removed by treatment with NaCN, affording the mononuclear bis-cyclotribenzylene complexes. These compounds failed to lead to metallo-cryptophanes by coordination of two $[M(dppp)]^{2+}$ complex subunits (M = Pd, Pt; dppp = 1,3-bis(diphenylphosphino)propane), each to two carbonitrile substituents belonging to different CTBs, pointing to the superiority of the one pot self-assembly processes for the preparation of metallo-cryptophanes.

Introduction

Metallo-cryptophanes[1] are analogues of the macropolycyclic compounds invented and subsequently developed by Collet and coworkers in the last two decades of the 20th century.[2] These hollow spheroidal compounds, which can exist in chiral versions, were shown to host a great variety of substrates, e.g., molecular, ionic, and even atomic, this last property being currently exploited for the development of biosensors and IRM probes based on hyperpolarized xenon.[3] In metallo-cryptophanes the usual organic bridges that connect two cyclotribenzylene (CTB) subunits in face-to-face configuration are replaced by metal complex subunits. For this purpose, it is necessary to design and synthesize CTB precursors bearing pendant ligand subunits. Thus CTBs with pyridyl,[4] carboxylate,[5] and carbonitrile[6] end groups have been reported, which, in combination with Pd^{II}-, Pt^{II}-, Ir^{III}-, and Ag^{I}-based metal complex subunits were shown to form a great variety of metallo-cryptophanes in terms of size by one-pot self-assembly reactions.

We recently used CTBs bearing carbonitrile groups for the Pd^{II}- and Pt^{II}-directed self-assembly of metallo-cryptophanes[6] with a size similar to those of the smallest organic cryptophanes that encapsulate haloalkanes, methane, and a xenon atom. The self-assembly proceeded under thermodynamic control, producing in some instances the chiral D_3-symmetric form diastereospecifically. In order to increase the robustness of these compounds, in particular with regard to dilution,[6b] we decided to replace one of the carbonitrile substituents by an isosteric alkyne substituent, which would allow us to make metallo-cryptophanes incorporating a kinetically inert *cis*-dialkynyl Pt^{II} bridge. The synthesis of such metallo-cryptophanes would involve two steps, first the preparation of the Pt-bridged CTB dimer, then its closure to a cryptophane by reaction with two equivalents of $[ML_2]^{2+}$ (M = Pd or Pt, L = PEt_3 or L_2 = dppp) complex subunits. Such a strategy resembles the approach for making organic cryptophanes of well-controlled cavity sizes by using bridges of different lengths.[7] In addition, the introduction of *cis*-(diarylalkynyl) Pt^{II} complex subunits would impart the metallo-cryptophane with interesting photophysical properties.[8] It is important to note that *cis*-(diarylalkynyl) Pt^{II}

[a] Dr. J. Zhang, Dr. F. Aribot, Dr. J.-C. Chambron
Institut de Chimie de Strasbourg
UMR 7177 CNRS
Université de Strasbourg
4, rue Blaise Pascal, 67070 Strasbourg (France)
E-mail: jcchambron@unistra.fr
[b] N. Zorn, Dr. E. Leize-Wagner
Chimie de la Matière Complexe
UMR 7140 CNRS
Université de Strasbourg
4, rue Blaise Pascal, 67070 Strasbourg (France)
E-mail: leize@unistra.fr
[c] M. Jean, Dr. N. Vanthuyne
Aix-Marseille Univ, CNRS
Centrale Marseille, iSm2
Marseille (France)
E-mail: nicolas.vanthuyne@univ-amu.fr
[d] Prof. Dr. E. Espinosa, Dr. E. Aubert
Université de Lorraine
CNRS, CRM2
F-54000 Nancy (France)
E-mail: emmanuel.aubert@univ-lorraine.fr

Supporting information for this article is available on the WWW under https://doi.org/10.1002/ejic.202300284

Research Article
doi.org/10.1002/ejic.202300284

complex subunits have been used as hinges for making tweezers-like receptors[9] or metallamacrocycles,[10] but this is the first time they are considered as potential assembling unit in molecular cages. In this report, we summarize our efforts towards such a challenging endeavor: The synthesis of C_1-symmetrical CTBs, their chiral resolution, their use in the preparation of Pt-bridged CTB dimers in enantiomerically pure form, and the attempts of the metal-complexation driven cyclization of the CTB dimers.

Results and Discussion

Synthesis, characterization, resolution, and absolute configurations of the asymmetric cyclotribenzylenes

The chemical structures of the enantiomers of the cyclotribenzylenes synthesized for and involved in these investigations are shown in Figure 1 with atom labelling. Compounds **1**H and **2**H are substituted CTBs, of which two γ′ positions bear a carbonitrile substituent, the third one bearing a terminal alkyne. The γ positions of **1**H are unsubstituted, while those of **2**H bear methoxy substituents. Remarkably, these compounds differ by their asymmetry from the classical CTBs of the literature, which are usually C_3-symmetric. **1**H and **2**H were prepared from known C_3-symmetric CTBs of the literature, namely CTB(H,OTf)[6a] and CTB(OMe,I),[11] respectively. In each case the desymmetrization, relying on a statistical distribution, was performed in the first step of the synthetic sequence. In the case of the preparation of **1**H (Scheme 1a), we chose to introduce the terminal alkyne first, via a copper-free Sonogashira coupling reaction.[12] Accordingly, CTB(H,OTf), which was prepared from CTB(H,OH), was reacted with trimethylsilylacetylene (1 equiv) in the presence of 25 mol% of $[Pd(PPh_3)_2Cl_2]$ catalyst and excess triethylamine at 50 °C overnight. Singly functionalized CTB **3** was separated by flash column chromatography from the di- and trisubstituted by-products (**3**′ and **3"**, respectively) and obtained in 30% isolated yield. In the next steps, we planned to introduce the carbonitrile substituents, then to remove the alkynyl protection. Therefore, **3** was reacted with $[Zn(CN)_2]$ in the presence of catalytic amounts of $[Pd(PPh_3)_4]$ and an excess of LiCl in DMF.[13] After 5 days stirring at 120 °C and purification by flash column chromatography, compound **1**H, in which the TMS protection had been removed, was obtained in 59% yield. The unanticipated deprotection of the terminal alkyne by CN^- somewhat compensated the 17% overall yield obtained in the preparation of unsymmetrical CTB **1**H from its symmetrical precursor. In the case of the preparation of CTB **2**H (Scheme 1b), preliminary experiments had shown that the reaction of CTB(OMe,I) with trimethylsilylacetylene had led to difficult chromatographic separations. Therefore we reversed the order of steps, and first reacted CTB(OMe,I) with $[Zn(CN)_2]$ in the same conditions as for the preparation of **1**H,[14] except that the reaction was stopped after 2 hours heating. Column chromatography led to the isolation of the desired disubstituted CTB intermediate **4** in 35% yield, alongside the singly substituted derivative **4**′, which was obtained in 21% yield. Next the aryliodide **4** was reacted, in Sonogashira conditions,[15] for 2 hours at 40 °C with an excess of trimethylsilylacetylene in the presence of 25 mol% of $[Pd(PPh_3)_2Cl_2]$ catalyst, 30 mol% CuI cocatalyst, and an excess of triethylamine. Compound **5** was obtained in 95% yield after column chromatography. The target CTB **2**H was readily obtained in 97% yield by reaction of **5** with an excess of tetrabutylammonium fluoride in THF at room temperature.

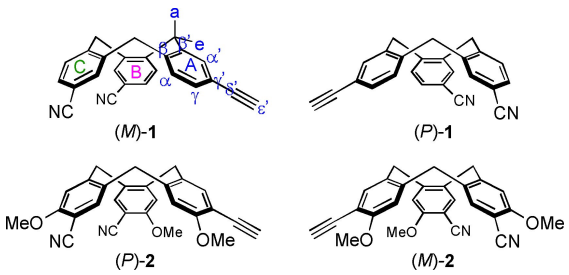

Figure 1. Structural formulae of the enantiomers of the cyclotribenzylenes (CTB) of this study. Protons labels are indicated for cycle A. They should be read α_A, etc. for cycle A, α_B, etc. for cycle B, etc. For the sake of simplicity colors are used in the figures: A, blue; B, magenta; C, green.

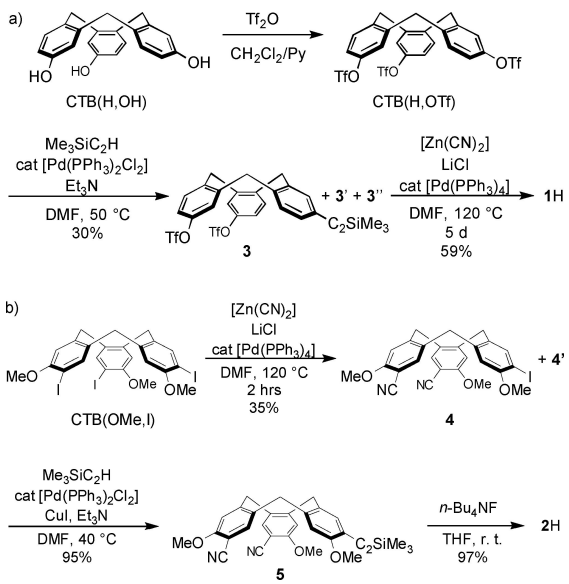

Scheme 1. Synthetic steps leading to (a) CTB **1**H and (b) CTB **2**H from known CTB precursors, respectively CTB(H,OH) and CTB(OMe,I).

1H and **2**H were characterized by ^1H and ^{13}C NMR spectroscopy, as well as IR spectrophotometry. Their NMR spectra are more complex than those of their C_3-symmetric precursors, as all three constitutive benzene rings are different (Figure 2 and Figures S1–S11). Therefore, each proton and each carbon atom showed its own signal, and it was necessary to perform 2D homonuclear (COSY and N(R)OESY) as well as heteronuclear (HSQC and HMBC) experiments to be able to assign all the NMR signals. The key NOESY correlations are those within the three proton triads (α-H, e-H, α′-H); the β, β′, γ′, δ′, and ε'_A-C carbon atoms are identified through the 3-bond ^{13}C-^1H correlations. Noteworthy, because of the asymmetry of the molecules, the dipolar couplings within the triad a-H can be

Research Article
doi.org/10.1002/ejic.202300284

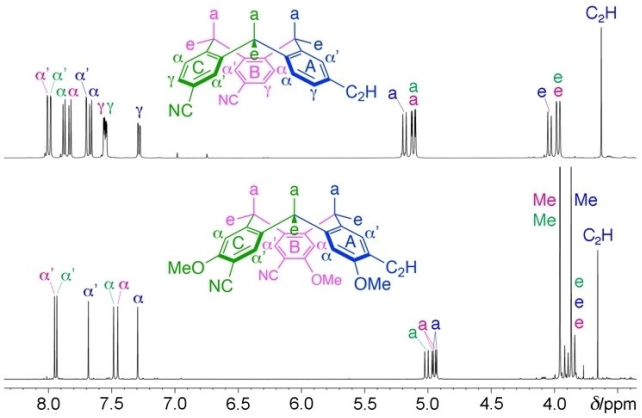

Figure 2. ^{1}H NMR spectra (500 MHz, $[D]_6$-acetone, 300 K) of (a) CTB **1**H and (b) CTB **2**H (structures of (*M*)-**1**H and (*P*)-**2**H shown). Ring A: labels in blue; ring B: labels in magenta; ring C: labels in green.

seen in the ROESY maps of **1**H and **2**H (see Figure S3, for example). The signals of the terminal carbon and proton at 79.26 and 3.629 ppm, and 79.59 and 3.272 ppm, for **1**H and **2**H, respectively, attest to the presence of a single alkynyl substituent. The IR spectra show a sharp absorption at 2227 (**1**H) and 2224 cm^{-1} (**2**H) due to the C≡N bond of the carbonitrile substituents, and a very weak absorption at 2104 (**1**H) and 2103 (**2**H) cm^{-1} due to the C≡C bond of the alkyne substituent.

The asymmetry of the CTBs **1**H and **2**H was probed by analytical HPLC on chiral phases coupled with UV and ECD detection. The chromatograms obtained showed two well separated signals, which exhibited opposite ECDs (Figures S12 and S14). Preparative HPLC on (*S*,*S*)-Whelk-O1 and elution with heptane/CH_2Cl_2 30:70 for **1**H, and heptane/CH_2Cl_2/ethanol 30:60:10 for **2**H, allowed us to separate, in good yields and ee's, (+)-**1**H and (−)-**1**H, on the one hand, (+)-**2**H and (−)-**2**H, on the other hand. In both cases the first eluted compound was the dextrorotatory enantiomer. The optical rotations at 365 nm measured for (+)-**1**H were much higher than those measured for (+)-**2**H, e.g +2530 (CH_2Cl_2, $c = 0.06$), *vs.* +241 (CH_2Cl_2, $c = 0.07$), while the kinetics of enantiomerization, run in chloroform, gave quasi-identical results (Figures S13 and S15): The half-life $t_{1/2}$ of an optically pure sample in chloroform at 62 °C was 204 min, and the corresponding barrier for enantiomerization was 111.6 kJmol^{-1} (26.7 kcal mol^{-1}). These values are in keeping with the values reported for substituted CTBs, and confirm again that the influence of the substituents on the enantiomerization barrier is negligible.[2b] The electronic absorption spectra of the enantiomers of **1**H (Figure S16) showed a broad band in the UV with a maximum at 244 nm ($\varepsilon = 47000$ $M^{-1}cm^{-1}$) and a tail extending between 265 and 295 nm, and maximizing at 278 nm ($\varepsilon = 2191$ $M^{-1}cm^{-1}$). By contrast, those of **2**H showed two bands, one in the same UV region as **1**H, with a maximum at 245 nm ($\varepsilon = 36700$ $M^{-1}cm^{-1}$), the other at lower energy, with a maximum at 311 nm and a lower molar extinction coefficient ($\varepsilon = 14200$ $M^{-1}cm^{-1}$). Whereas the high energy UV absorption of **1**H and **2**H is likely to correspond to the B_{1u} region of the phenyl ring, the low energy UV absorption of **2**H could correspond to the π*←n transition originating from the methoxy substituents and overlapping with the B_{2u} transition of the phenyl ring.[16] The ECD of (+)-**1**H (Figure 3) shows a bisignate band extending down to 267 nm, with maxima and minima at 235 ($\Delta\varepsilon = +93.8$ $M^{-1}cm^{-1}$) and 252 nm ($\Delta\varepsilon = -33.5$ $M^{-1}cm^{-1}$), sign inversion at 248 nm, and a singly signed band with a low $\Delta\varepsilon_{max}$ of 7.67 $M^{-1}cm^{-1}$ at 288 nm. This spectrum is similar to the ECD spectrum of the C_3-symmetric CTB(H,CN) analogue of **1**H, which bears three carbonitrile substituents.[6b] The ECD of (+)-**2**H shows the fragment of a negative band down to 230 nm, then a bisignate band from 230 to 281 nm, with maxima and minima at 239 ($\Delta\varepsilon = +55.7$ $M^{-1}cm^{-1}$) and 261 nm ($\Delta\varepsilon = -27.8$ $M^{-1}cm^{-1}$) and sign inversion at 252 nm. The value of 281 nm seems also to be the high energy limit of a second bisigned band showing first a minimum at 295 nm ($\Delta\varepsilon = -11.0$ $M^{-1}cm^{-1}$), then a maximum at 314 nm ($\Delta\varepsilon = +20.5$ $M^{-1}cm^{-1}$), which are separated by the point of sign inversion at 304 nm. This latter band is likely to be associated with the π*←n transition identified in the electronic absorption spectrum.

Collet and Gottarelli applied the exciton model of optical activity to C_3-symmetric cyclotriveratrylenes in particular.[17] They demonstrated that this model, combined with the Platt's spectroscopic moment theory, could be used for the assignment of absolute configurations, as the shapes of the calculated spectra matched well with those of the experimental ones. The CTBs of the present study being asymmetric, we preferred to carry out ab-initio TD-DFT calculations. They were performed at the CAM-B3LYP-D3 level of theory, using the 6-311+G(d,p) functional, and took into account the effects of the solvent (CH_2Cl_2). They allowed us to calculate the optical rotations at the experimental wavelengths, as well as the ECD spectra. In the case of **1**H, the calculations were performed for the *M* configuration (Figure S17) and were straightforward. The portion of the calculated ECD spectrum corresponding to the B_{1u} region of the electronic absorption spectrum (Figure S18) matched very well with the experimental spectrum of (+)-**1**H, which showed that the absolute configurations of (+)-**1**H and (−)-**1**H were *M* and *P*, respectively. The quality of the calculations was confirmed by the good correspondence and

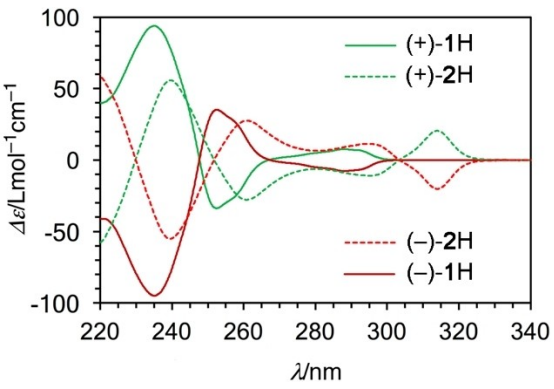

Figure 3. Experimental ECD spectra of the enantiomers of CTBs **1**H and **2**H in CH_2Cl_2.

Research Article
doi.org/10.1002/ejic.202300284

the linear correlation between the theoretical and the experimental optical rotations (Figure S19). In the case of **2**H, the calculations were complicated by the fact that the molecule can adopt different conformations, which result from different orientations of the methyl group of the methoxy substituents, either towards the inside (i) or towards the outside (o) of the molecular concavity. They give rise to secondary energy minima as already noted in the case of related compounds.[18] Eight conformations were identified: ooo and iii, on the one hand, ioo, oio, ooi, iio, ioi, and oii, on the other hand (Figure S20). After optimization of the structures, calculation of the energies, and determination of the distribution of the Boltzmann populations of these conformations (Table S1), their ECD spectra were calculated, as well as the ECD spectrum of their weighted superposition (Figure S21). The spectrum calculated for the *P* configuration (Figure S22) matched well with the experimental spectrum recorded for (+)-**2**H in the B_{1u} region. This assignment was confirmed by the calculation of the optical rotations of (*P*)-**2**H (Table S2), which were all positive, whatever the conformation; however, unlike (*M*)-**1**H, the magnitudes of the calculated $[\alpha]^{25}_{\lambda}$ were very much higher than their experimental counterpart, and they were not linearly correlated. We found also that the absorption band at 314 nm was not confirmed by the calculations.

In conclusion, opposite configurations of **1**H and **2**H have the same sign of optical rotation, the absolute configurations of (+)-**1**H and (+)-**2**H being *M* and *P*, respectively.

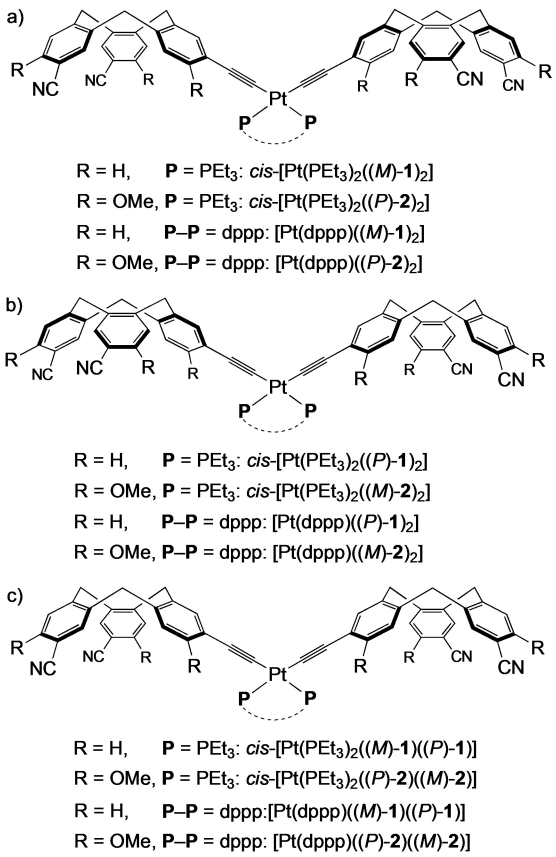

Figure 4. Structural formulae and absolute configurations of the (a and b) *anti* and (c) *syn* diastereoisomers of the CTB dimers [*cis*-$Pt(PEt_3)_2$(**1**)$_2$], [*cis*-$Pt(PEt_3)_2$(**2**)$_2$], [Pt(dppp)(**1**)$_2$], and [Pt(dppp)(**2**)$_2$] (dppp is 1,3-bis(diphenylphosphino)propane).

Preparation of the Pt^{II}-Bridged CTB dimers

The structures of the four platinum bis-alkynyl complexes of this study and their *anti* and *syn* diastereoisomers are displayed in Figure 4. We used two different ancillary ligands for the Pt^{2+} cation, either two single donor atom PEt_3 phosphine ligands predisposed in *cis* configuration, or a diphosphine chelate (dppp = 1,3-bis(diphenylphosphino)propane), for the preparation of the neutral complexes *cis*-[$Pt(PEt_3)_2$(**1**)$_2$], [Pt(dppp)(**1**)$_2$], *cis*-[$Pt(PEt_3)_2$(**2**)$_2$], and [Pt(dppp)(**2**)$_2$]. Following the original report by Sonogashira, Hagihara and coworkers,[19] the complexes were prepared by the copper(I)-catalyzed dehydrohalogenation coupling reaction of the appropriate *cis*-[PtL_2Cl_2] precursor (L = PEt_3 or L_2 = dppp) with the alkyne-functionalized CTBs in racemic or optically pure form in the presence of a base (NEt_3) and CuI. In the first case diastereoisomeric mixtures of the achiral *syn* form and chiral *anti* forms were obtained, in the second case, enantiomerically pure CTB dimers were isolated. They were characterized in solution by ESI mass spectrometry and by NMR spectroscopy (^{1}H, ^{13}C, and ^{31}P), the signals of the ^{1}H and ^{13}C NMR spectra being assigned by a combination of ^{1}H/^{1}H ROESY, ^{13}C/^{1}H HSQC and ^{13}C/^{1}H HMBC 2D techniques. Assignment of the NMR spectra of the mixtures of the *anti* and *syn* diastereoisomers was performed using the corresponding data obtained for one of the *anti* diastereoisomers, either prepared from an enantiopure CTB or obtained by preparative HPLC on a chiral phase.

Preparation and characterization of the platinum complexes deriving from CTB 1H

Reaction of *rac*-**1**H with *cis*-[$Pt(PEt_3)_2Cl_2$] in 2:1 ratio in THF at room temperature in the presence of 40 mol% CuI (with respect to Pt) and Et_3N in excess afforded, after aqueous workup and silicagel column chromatography, *cis*-[$Pt(PEt_3)_2$(**1**)$_2$] in 48% yield, as a 1:1 mixture of *syn* and *anti* diastereoisomers (Figures S23–S27). In the ^{1}H NMR spectrum the most deshielded signals of the CTB aromatic protons (*ca.* 7.94 ppm) were those of the α'_B and α'_C protons *ortho* to the –CN functions, while the most shielded (7.07 ppm) were the overlapping dd signals of the γ_A protons *ortho* to the metal-bound alkynyl functions. For a collision energy (E_{coll}) ≥ 100 eV, the ESI mass spectrum of the mixture of diastereoisomers (Figure S28) showed a major signal at *m/z* 1140.38, which corresponds to the molecular sodium adduct ($[M+Na]^+$), and a signal of lower intensity at *m/z* 2257.78, which corresponds to the sodium adduct of the molecular dimer ($[2\,M+Na]^+$). Both exhibited the expected isotopic profile (Figure S29). In the same conditions, the reaction of *rac*-**1**H with [$Pt(dppp)Cl_2$] afforded, after purification, [Pt(dppp)$_2$(**1**)$_2$] in 27% yield, again as the expected 1:1 mixture of *syn* and *anti* diastereomers (Figures S30–S34). The signals of

Research Article
doi.org/10.1002/ejic.202300284

the α'_B and α'_C protons were also the most deshielded of the CTB component (at *ca.* 7.62 ppm), but to a lesser extent than in the case of *cis*-[Pt(PEt$_3$)$_2$(**1**)$_2$]. The dd signals of the γ_A protons were well separated and were shielded by 0.61 ppm by comparison with their homologs in *cis*-[Pt(PEt$_3$)$_2$(**1**)$_2$]. This shielding could be due to the proximity of one of the phenyl substituents of the dppp ligand (see the insert of Figure 5). Once again, the ESI mass spectrum of the product showed the signal of the sodium molecular adduct at *m/z* 1316.35 with the expected isotopic profiles (Figures S35–S37). It was the major one only at $E_{coll} \geq 150$ eV. Below this value, the major signal was observed at *m/z* 1379.37, the origin of which is unclear.

The enantiomerically pure *anti* complexes [Pt(dppp)((−)-**1**)$_2$] and [Pt(dppp)((+)-**1**)$_2$] were prepared separately from the corresponding enantiomerically pure CTBs. They were obtained in 54% and 34% yields, respectively, after column chromatography on silicagel. The ^{1}H NMR spectra of these complexes are, as expected, identical. Moreover, they do not show any trace of *meso* form, which indicates that the CTBs did not racemize in the course of the preparation. As an illustration, the ^{1}H NMR spectrum of [Pt(dppp)((−)-**1**)$_2$] is displayed in Figure 5 (complete assignment: Figures S38–S44). Comparison with the corresponding spectrum of [Pt(dppp)$_2$(**1**)$_2$] (Figures S30–S34) shows that the signals of the protons of the *syn* diastereoisomer are not strongly shifted with respect to those of the enantiomers of the *anti* diastereoisomer. In particular, the signals of the axial and the equatorial protons seem to be superimposed. Remarkably, the [$C_{(\varepsilon'A)}$—Pt—P($C_{(i)}C_5H_6$)$_2$—$CH_{(r)2}$] sequence could be identified in the 2D ^{13}C/^{1}H HMBC map as the four-bond correlation ε'_A-C/r-H (Figure S44). It is complemented by the $^2J_{C,P}$ couplings ε'_A-C/*cis*-P = 22 Hz and ε'_A-C/*trans*-P = 147 Hz. The ^{31}P NMR spectrum of [Pt(dppp)((+)-**1**)$_2$] showed a singlet at −5.97 ppm with two ^{195}Pt satellites ($^1J_{P,Pt}$ = 2188 Hz, Figure S40), values that are in keeping with literature data.[20] The ESI mass spectrum of [Pt(dppp)((−)-**1**)$_2$] (Figure S45) showed very weak signals of the proton and sodium molecular adducts, respectively at *m/z* 1294.35 (I_{rel} = 0.45) and *m/z* 1316.35 (I_{rel} = 1.00) when E_{coll} = 20 eV. The signal of the doubly charged species, corresponding to the ion [2 M + 2Na]$^+$ was superposed to the signal of [M + Na]$^+$. It presumably corresponded to an artifact as upon rinsing the capillary only the signal of [M + Na]$^+$ was observed.

The electronic spectroscopy and chiroptical properties of the complexes [Pt(dppp)((+)-**1**)$_2$] and [Pt(dppp)((−)-**1**)$_2$] were investigated in dichloromethane solution. Optical rotations

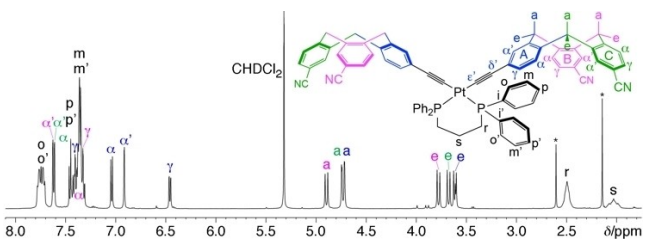

Figure 5. ^{1}H NMR spectrum (500 MHz, CD_2Cl_2, 300 K) of [Pt(dppp)((−)-(*P*)-**1**)$_2$] (✱: solvent impurity). Ring A: labels in blue; ring B: labels in magenta; ring C: labels in green.

(Table S1) of [Pt(dppp)((+)-**1**)$_2$], which was prepared from (+)-**1**H, ranged from + 340 at 589 nm to + 1180 at 405 nm, and are therefore of lower magnitude than those corresponding to (+)-**1**H (respectively + 595 and + 1690). Opposite values were recorded for [Pt(dppp)((−)-**1**)$_2$], which was prepared from (−)-**1**H. The electronic absorption spectra of [Pt(dppp)((+)-**1**)$_2$] and of its precursor (+)-**1**H are displayed in Figure S46. Whereas, as seen earlier, **1**H shows an absorption band centered at 244 nm, the complex [Pt(dppp)((−)-**1**)$_2$] shows multiple absorption bands between 220 and 360 nm with a shoulder at 232 nm (ε = 65200 M^{-1}cm^{-1}), and maxima at 275 (ε = 27600 M^{-1}cm^{-1}) and 318 nm (ε = 21500 M^{-1}cm^{-1}). The ECD spectra of [Pt(dppp)((+)-**1**)$_2$] and [Pt(dppp)((−)-**1**)$_2$] (Figure S47) do not show any bisignate pattern between 220 and 360 nm, contrary to those of the corresponding CTBs (+)-**1** and (−)-**1**, but broad absorptions with positive maxima at 235 ($\Delta\varepsilon$ = 67 M^{-1}cm^{-1}), 288 ($\Delta\varepsilon$ = 7.7 M^{-1}cm^{-1}), and 325 nm ($\Delta\varepsilon$ = 16.5 M^{-1}cm^{-1}) for [Pt(dppp)((+)-**1**)$_2$] and negative maxima for [Pt(dppp)((−)-**1**)$_2$]. A similar spectrum had been observed in the case of the platinocryptophane [Pt$_3$(dppp)$_3$(CTB(H,CN))$_2$]$^{6+}$ made from the C_3-symmetric carbonitrile-substituted CTB(H,CN).[6b]

Preparation and characterization of the platinum complexes deriving from CTB 2H

Complexes based on the cis-[Pt(PEt$_3$)$_2$]$^{2+}$ assembling unit

The crude product of the reaction of *rac*-**2**H with *cis*-[Pt(PEt$_3$)$_2$Cl$_2$] in 2:1 ratio in the presence of 41 mol% CuI with respect to Pt and excess Et$_3$N in DMF at room temperature for 3 days was controlled by ^{1}H NMR spectroscopy before work-up and purification. By contrast with what we observed in the experiments involving CTB **1**H, the spectrum showed, in particular, two low field singlets at 8.52 and 8.41 ppm, respectively, that corresponded to the α'_A protons of two products in 1:1 ratio (Figure S48). The crude was purified by column chromatography on silicagel, and the different fractions examined by ^{1}H NMR spectroscopy. The less polar product was the singly substituted platinum complex, [Pt(PEt$_3$)(**2**)Cl], the spectrum of which was very similar to the one of **2**H; the subsequent fractions contained a mixture of two products, the ratio between the diastereoisomers changing in the course of the chromatographic separation, the most polar being the one exhibiting the most deshielded α'_A protons. The last fractions contained exclusively the most polar product in minor amounts. The set of fractions that were collected for complete NMR characterization (Figures S49–S55) had a ratio of 66:34 between the more polar (*anti*) and the less polar (*syn*) product. The yield of the isolated mixture of diastereoisomers in pure form was 50%. These products were examined by Q-Tof ESI-MS. At an ionization energy (*IE*) of 30 eV, signals were observed at *m/z* 1320.45, 1360.39, and 1418.35 in 50:17:33 ratio. They corresponded to the molecular ions [M + Na]$^+$, [M + Cu]$^+$, and [M + CuCl + Na]$^+$, respectively. At *IE* = 50 eV, there remained only the signal corresponding to [M + Cu]$^+$ (Figures S56–S57). DOSY experiments allowed us to compare the diffusion coefficients of

Research Article
doi.org/10.1002/ejic.202300284

Chemistry Europe
European Chemical Societies Publishing

2H and of the diastereoisomeric complexes (Figure S58): $D = 9.74 \times 10^{-10}$ m^2 s^{-1} for the former, and $D = 6.10 \times 10^{-10}$ m^2 s^{-1} for the latter, which is in qualitative agreement with the expected increase of size on going from the CTB to the platinum-bridged CTB dimer. Further use of the DOSY information will be provided in a next section.

Comparison of the proton NMR spectra of **2**H and of its reaction product with *cis*-[Pt(PEt$_3$)$_2$Cl$_2$] and CuI in CD_2Cl_2 is shown in Figure 6a,b. In the latter, the CTB signals are splitted in two, each set corresponding to a diastereoisomer (*syn* and *anti*), respectively. Note that we use embolded symbols for labelling the subspectra of the *anti* diastereoisomers throughout this report. The effect of the substitution of the *cis*-[Pt(PEt$_3$)$_2$]$^{2+}$ moiety for the alkynyl proton of **2**H is the following: In the aromatic region, the signals of protons α_A, α'_B, and α'_C show only small shifts, whereas those of protons α_B and α'_A undergo significant downfield shifts, whatever the diastereoisomer considered. In the aliphatic region, the chemical shifts of the signals of the methoxy protons Me_B and Me_C of the *syn*-diastereoisomer are very close to those of **2**H, whereas the signals of the methoxy protons Me_A and Me_B of the *anti*-diastereoisomer are significantly shielded and deshielded, respectively. The $^{31}P\{^1H\}$ NMR spectrum of the diastereoisomeric mixture (Figure S50) showed two singlets, at 4.18 and 4.23 ppm with two ^{195}Pt satellites ($^1J_{P,Pt} = 2495$ Hz). Noteworthy is the fact that the ^{1}H NMR spectra of the mixture of diastereoisomers are solvent-, concentration-, and temperature-dependent: Details are provided in the Supporting Information p. S5 and in Figures S59–S63.

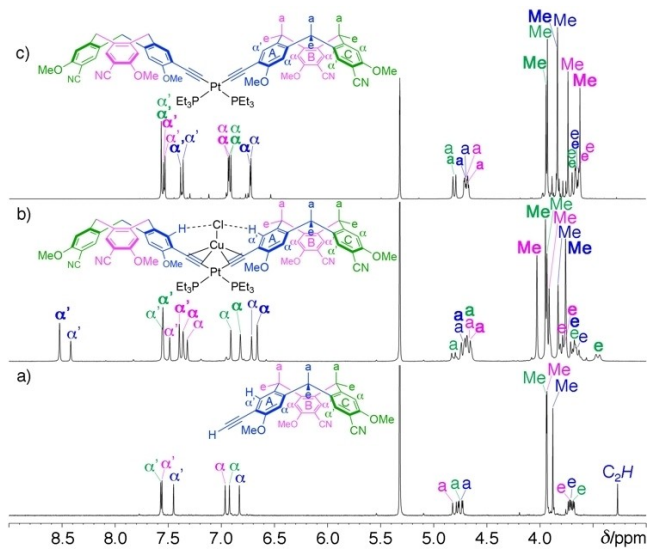

Figure 6. Stacked plot of the ^{1}H NMR spectra (400 MHz, CD_2Cl_2, 298 K) of (a) CTB **2**H (structure of (*M*)-**2**H shown), (b) the diastereoisomeric mixture of the complexes *syn*- and *anti, cis*-[Pt(PEt$_3$)$_2$(**2**)$_2$CuCl] (structure of *anti*, *cis*-[Pt(PEt$_3$)$_2$((*M*)-**2**)$_2$CuCl] shown), and (c) the diastereoisomeric mixture of the complexes *syn*- and *anti, cis*-[Pt(PEt$_3$)$_2$(**2**)$_2$] (structure of *anti*, *cis*-[Pt(PEt$_3$)$_2$((*M*)-**2**)$_2$] shown). Ring A: labels in blue; ring B: labels in magenta; ring C: labels in green. The embolded labels mark signals of the *anti* diastereoisomers in (b) and (c).

Based on the large *ca.* +1 ppm downfield shift of the signals of the α'_A protons of both diastereoisomers, the mass spectrometry results, and the concentration dependence of their ^{1}H NMR spectra, we suggest that the Pt complexes obtained in the conditions described in this section could be formulated as *cis*-[Pt(PEt$_3$)$_2$(**2**)$_2$CuCl], in which CuCl is bound in η^2-fashion to each alkynyl bridge (insert of Figure 6b). In this way, the metal-coordinated halide ion could interact with the proximal α'_A protons of the CTB subunits via Ar–H···Cl hydrogen bonding, which would explain the sizeable deshielding of α'_A by comparison with α'_B and α'_C. Further evidence of the CuCl coordination could be provided by the estimation of the molar mass of *cis*-[Pt(PEt$_3$)$_2$(**2**)$_2$CuCl] according to Equation (1):

$$M_A = M_B(D_B/D_A)^3 \quad (1)$$

where M_A is the molar mass of the CTB dimer, M_B the molar mass of **2**H, and D_A and D_B the corresponding diffusion coefficients. Using the values obtained from the DOSY measurements and the molar mass of **2**H we obtain $M_A = 1769$ gmol^{-1}, which is 27% (36%) higher than the 1397.35 gmol^{-1} (1298.38) value expected for *cis*-[Pt(PEt$_3$)$_2$(**2**)$_2$CuCl] (*cis*-[Pt(PEt$_3$)$_2$(**2**)$_2$]), respectively.

Such a "spontaneous", somewhat unexpected CuCl adduct formation by π-coordination to the triple bonds of alkynyl ligands bound to a *cis*-platinum metal complex fragment had been already observed,[21] for example in the course of the preparations of [Pt(dppe)(C$_2$Ph)$_2$],[21a] [Pt(Mes–BIAN)(C$_2$SiMe$_3$)$_2$],[21b] and the metallamacrocycle *cis*-[Pt(PEt$_3$)$_2$L], in which L is a bis-alkyne chelate.[21c] Besides, binuclear complexes [LM(C$_2$R)$_2$-η^2,η^2-M′X] based on bis-alkynyl pincer complexes [LM(C$_2$R)$_2$] with σ M–C bonds have been known for quite a long time.[22] Direct evidence of M′X binding to the bis-alkynyl π-tweezers was provided in all cases in the solid state by an X-ray crystallography study. In solution, binding of CuCl to *cis*-[Pt(dppe)(C$_2$Ph)$_2$] for example, had little effect on the ^{31}P NMR chemical shift ($\Delta\delta = -3$%) and no effect on the alkynyl ^{13}C NMR chemical shifts;[21a] +FAB mass spectrometry of [Pt(*t*Bu$_2$bipy)(C≡CC$_6$H$_4$Me)$_2$Cu(SCN)] gave the signal corresponding to [M–SCN$^-$]$^+$.[22d] We note that such a hydrogen bond with a metal-bound halide has been recently observed in platinum indolylphosphine fluorido and chlorido complexes, with strong deshielding of the hydrogen-bound N*H* protons.[23]

To test further the hypothesis of copper(I) coordination, the crude product of the reaction of *rac*-**2**H with *cis*-[Pt(PEt$_3$)$_2$Cl$_2$] in 2:1 ratio in the presence of 21 mol% CuI and excess Et$_3$N was, after removal of the volatile species, treated with the stoichiometric amount of NaCN prior to purification by column chromatography on silicagel. Figure S64 compares the ^{1}H NMR spectra in $CDCl_3$ of the crude product before and after treatment by NaCN, so that the diastereoisomeric ratio is the same in both samples. The complex *cis*-[Pt(PEt$_3$)$_2$(**2**)$_2$CuCl] was diluted, hence, as could be inferred from the trends observed in Figure S60, the *syn* and *anti* diastereoisomers had nearly superimposable spectra, except for the signals of protons α'_A and α_B, that is, the protons that are directly bound and very close to the chloride anion, respectively. The *anti* diastereoisomers of

Research Article
doi.org/10.1002/ejic.202300284

cis-[Pt(PEt$_3$)$_2$(**2**)$_2$CuCl] and *cis*-[Pt(PEt$_3$)$_2$(**2**)$_2$] are characterized by the most deshielded α'_A and most shielded Me$_B$ protons respectively in their ^{1}H NMR spectra (CD_2Cl_2: Figure 6b,c; $CDCl_3$: Figure S64a,b). Therefore, upon going from *cis*-[Pt(PEt$_3$)$_2$(**2**)$_2$CuCl] to *cis*-[Pt(PEt$_3$)$_2$(**2**)$_2$], whereas, whatever diastereoisomer considered, the signals of the protons α'_C, α'_B, α_C, α_A, Me$_A$, and Me$_C$, did not show significant shifts, the major differences concerned the signals of the protons α'_A, α_B, and Me$_B$, which were shifted upfield in both diastereoisomers, the signal of α'_A-H exhibiting the strongest shift (>1 ppm). The product *cis*-[Pt(PEt$_3$)$_2$(**2**)$_2$] was obtained in 65% yield as a mixture of diastereoisomers (in 56:44 *syn*/*anti d.r.*) as confirmed by TLC, ^{1}H, ^{13}C, and ^{31}P NMR spectroscopy (Figures S65–S72). In particular, the ^{31}P NMR spectrum in $C_2D_2Cl_4$ solution (Figure S67) showed two close singlets at 4.37 and 4.32 ppm with $^1J_{P,Pt}$ = 2254 Hz. In the ^{13}C NMR spectrum, the signals of the alkynyl carbon atoms δ'_A (t, $^3J_{C,P}$ = 16.5 Hz) and ε'_A (dd, $^2J_{cis\text{-}C,P}$ = 21.8 Hz, $^2J_{trans\text{-}C,P}$ = 142.5 Hz) of both diastereoisomers could be identified owing to the ^{13}C/^{1}H HMBC correlations with the methyl protons of the PEt$_3$ co-ligands (Figure S72). The ESI-MS spectrum of *cis*-[Pt(PEt$_3$)$_2$(**2**)$_2$] showed the signals of the proton (*m/z* 1298.47) and sodium (*m/z* 1320.45) molecular adducts in ratios depending on E_{coll} and the ion (E_{ion}) energy (41:59 for E_{coll} = 50 eV and E_{ion} = 5 eV; 57:43 for E_{coll} = 5 eV and E_{ion} = 40 V), with the expected isotopic distribution (Figures S73–S75).

Analysis of the changes of the ^{1}H NMR spectra in $CDCl_3$ upon going from **2**H to the diastereoisomeric mixture of *cis*-[Pt(PEt$_3$)$_2$(**2**)$_2$] is also quite interesting (Figure S76). In the aromatic region, only the signals of the protons α_A and α_B are affected significantly, being upfield shifted. In the aliphatic region, the most important changes concern the signals of the Me$_B$ protons (the Me$_A$ protons also, albeit to a lesser extent), which are shifted upfield by −0.56 ppm for the *anti* diastereoisomer and −0.23 ppm for the *syn* diastereoisomer. In fact, as illustrated in Figure S77, whereas the chemical shift of the Me$_B$ signal of the *syn* diastereoisomer was solvent independent (3.71 ppm in $CDCl_3$, 3.74 ppm in CD_2Cl_2, and 3.73 ppm in $C_2D_2Cl_4$), this was not the case of the chemical shift of the Me$_B$ signal of the *anti* diastereoisomer: 3.39 ppm in $CDCl_3$, 3.62 ppm in CD_2Cl_2, and 3.70 ppm in $C_2D_2Cl_4$. In this last solvent, the Me$_B$ protons of the two diastereoisomers experience similar magnetic fields. We shall see that the upfield shift of the Me$_B$ protons *vs.* their Me$_A$ and Me$_C$ counterparts is a general characteristics of the copper-free CTB dimers, whatever the nature of the phosphine ancillary ligand, and that it will allow us to outline the conformation of these complexes.

The NMR fingerprints of the *syn* and *anti* configurations of the diastereoisomers of *cis*-[Pt(PEt$_3$)$_2$(**2**)$_2$CuCl] and *cis*-[Pt(PEt$_3$)$_2$(**2**)$_2$] were then established by preparing the enantiomerically pure complexes *cis*-[Pt(PEt$_3$)$_2$((−)-**2**)$_2$CuCl] and *cis*-[Pt(PEt$_3$)$_2$((−)-**2**)$_2$], and comparing their NMR spectra to those of the corresponding diastereoisomeric mixtures, details being given in the Supporting Information p. S5 and in Figures S78–S80.

Complexes based on the [Pt(dppp)]$^{2+}$ assembling unit

The reaction of the CTB racemate **2**H and [Pt(dppp)Cl$_2$] in 2:1 ratio with less CuI loading than previously used (*ca.* 15 mol%) but still excess Et$_3$N and for three days at room temperature allowed us to obtain both diastereoisomeric mixtures of [Pt(dppp)(**2**)$_2$] (in 57:43 *d.r.*) and [Pt(dppp)(**2**)$_2$CuCl] (in 67:33 *anti*/*syn d.r.*), as shown by the ^{1}H NMR spectrum of the crude product (Figure S81). They were separated by column chromatography and isolated in 32 and 31% yields, respectively. Their ESI-MS spectra are shown in Figures S82–S86 and their complete set of NMR spectra are shown in Figures S87–S106. Details are reported in the Supporting Information p. S6. The ^{1}H NMR spectrum in $CDCl_3$ of the pure diastereoisomeric mixture of [Pt(dppp)(**2**)$_2$] is displayed together with the spectrum of **2**H in Figure 7. The comparison shows that the complexation of [Pt(dppp)]$^{2+}$ to the CTB **2**$^-$ subunits induces significant upfield shifts of several protons in both diastereoisomers. In the aromatic region of the spectrum, the most affected signals are those of α'_A, α_A, and α_B-H; in the high field region, the most affected are the signals of a$_A$ and e$_A$, a$_B$ and e$_B$-H, Me$_A$ and Me$_B$, the Me$_B$ signal of the *anti* diastereoisomer being more shifted ($\Delta\delta$ = −0.51 ppm) than the one of the *syn* ($\Delta\delta$ = −0.36 ppm). In CD_2Cl_2, the Me$_B$ signal is shielded by $\Delta\delta$ = −0.31 ppm and −0.20 ppm for the *anti* and *syn* diastereoisomers, respectively. The solvent-dependence of the ^{1}H NMR spectra of the diastereoisomers of [Pt(dppp)(**2**)$_2$] is illustrated in Figure S96.

Examination of the ^{1}H NMR spectrum of the diastereoisomeric mixture of [Pt(dppp)(**2**)$_2$CuCl] that was strongly enriched in the *anti* diastereoisomer (83:17 *anti*/*syn d.r.*) shows, by comparison with the spectrum of the diastereoisomeric mixture of *anti*- and *syn*-[Pt(dppp)(**2**)$_2$] (Figure S106), that the strong downfield shift of the signals of α'_A that was previously observed in the case of [Pt(PEt$_3$)$_2$(**2**)$_2$CuCl] is also observed in the case of [Pt(dppp)(**2**)$_2$CuCl], pointing to the same mode of bonding of the CuCl complex fragment. A noticeable difference

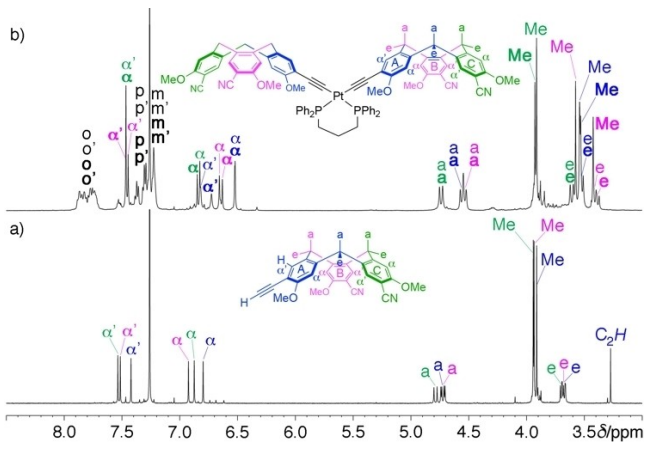

Figure 7. Stacked plot of the ^{1}H NMR spectra ($CDCl_3$, 400 MHz, 298 K) of (a) CTB **2**H and (b) the diastereoisomeric mixture of the complexes *syn*- and *anti*-[Pt(dppp)(**2**)$_2$] (structures of (*M*)-**2**H and *anti*-[Pt(dppp)((*M*)-**2**)$_2$] shown). Ring A: labels in blue; ring B: labels in magenta; ring C: labels in green. The embolded labels mark signals of the *anti* diastereoisomers.

Research Article
doi.org/10.1002/ejic.202300284

however is the strong upfield shift of the signals of the methoxy Me_A protons, which is probably due to the shielding of these protons by one of the phenyl substituents of the dppp ligand, the latter being closer to Me_A than the other methoxy substituents, as observed in the case of [Pt(dppp)(**2**)$_2$]. The same phenomenon could also explain why the α'_A protons are slightly less deshielded in [Pt(dppp)(**2**)$_2$CuCl] than in [Pt(PEt$_3$)$_2$(**2**)$_2$CuCl], the deshielding, due to hydrogen bonding to the chloride anion being thwarted by the shielding effect of the phenyl dppp substituents. Besides, the Me_B protons of both complexes undergo upfield shifts upon Cu^+ removal.

Direct evidence for the diastereoisomeric nature of [Pt(dppp)(**2**)$_2$CuCl] was obtained by chiral HPLC. The chromatogram showed three bands (Figure S107). The first two bands were nearly base-line separated, had similar areas (32.5 and 31.2%), and had CD signals of opposite signs; the third band partially overlapped with the second band, had an area of 36.3%, and did not show any CD. These analytical results are consistent with the fact that the mixture investigated contained two types of diastereoisomers, the two optically-active enantiomers (*anti* form) eluting first followed by the achiral diastereoisomer (*syn* or *meso* form). The pair of enantiomers could be separated from the *meso* form on an analytical column in sufficient amounts to record the ^{1}H NMR spectra of the diastereoisomers separately in CD_2Cl_2 (Figure S108). The *syn* diastereoisomer was characterized by the highest field signal of protons α'_A at $\delta = 8.09$ ppm, while the *anti* diastereoisomer showed the lowest field signal of protons α'_A at $\delta = 8.18$ ppm.

Interestingly, at highest CuI loading (50 mol%), we isolated, in addition to the already known diastereoisomeric mixture of the CuCl adduct, the one corresponding to [Pt(dppp)(**2**)$_2$CuI]. The ^{1}H NMR spectra in $CDCl_3$ of both diastereoisomeric mixtures are compared in Figure S109. [Pt(dppp)(**2**)$_2$CuI] was the less polar mixture of diastereoisomers. It showed (Figure S109a) shielded and deshielded singlets for the α'_A (8.27 and 8.08 ppm) and the Me_A (3.28 and 3.19 ppm) protons, respectively, by comparison with [Pt(dppp)(**2**)$_2$CuCl], the more polar mixture of diastereoisomers, which showed (Figure S109b) the opposite (for α'_A-H, $\delta = 8.33$ and 8.13 ppm; for Me_A, $\delta = 3.14$ and 3.07 ppm). The downfield shift (*ca.* +0.06 ppm) upon going from the CuI adduct to the CuCl adduct is consistent with the highest electronegativity of chloride by comparison with iodide. Evidence for the formulation of the CuI adduct was provided by its ESI-MS spectrum, which gave six peaks that corresponded to the following ions: *m/z* 1190.16 [{Pt(dppp)(**2**)Cl}+Na]$^+$, 1231.09 [{Pt(dppp)(**2**)Cl}+Cu]$^+$, 1497.40 [{Pt(dppp)(**2**)$_2$}+Na]$^+$, 1537.35 [{Pt(dppp)(**2**)$_2$}+Cu]$^+$, 1687.23 [{Pt(dppp)(**2**)$_2$CuI}+Na]$^+$, and 1727.17 [{Pt(dppp)(**2**)$_2$CuI}+Cu]$^+$. Their relative intensities depended on the *ISCID* and the E_{coll} (Figures S110–S113). Elemental analyses (see Experimental section) were also consistent with the less polar diastereoisomers incorporating CuI and the more polar diastereoisomers incorporating CuCl. The enantiomerically pure complex *anti*-[Pt(dppp)((+)-**2**)$_2$CuI] was obtained in 38% yield by reacting (+)-**2**H and [Pt(dppp)Cl$_2$] in 2:1 ratio in the presence of a nearly stoichiometric amount of CuI (83 mol%) and an excess of Et_3N in THF for three days at room temperature. Column chromatography also allowed us to isolate, as side-product in 18% yield, *anti*-[Pt(dppp)Cl((+)-**2**)], which was characterized by ^{1}H and ^{31}P NMR (Figures S114 and S115). The enantiomerically pure *anti*-[Pt(dppp)((+)-**2**)$_2$CuI] complex was fully characterized by NMR spectroscopy (Figures S116–S129), mass spectrometry (Figure S130), and electronic spectroscopy (Figure S131). The values of the optical rotations are collected in Table S5.

Subsequently, the complex *anti*-[Pt(dppp)((+)-**2**)$_2$] could be obtained by reaction of *anti*-[Pt(dppp)((+)-**2**)$_2$CuI] with an excess of NaCN (4 equiv) at 0 °C. A stacked plot of its ^{1}H NMR spectra in three different solvents ($CDCl_3$, CD_2Cl_2, and $C_2D_2Cl_4$) is shown in Figure S132. It can be seen that whereas the chemical shifts of the Me_C protons are solvent-independent, this is not the case of the Me_A and Me_B protons, which are increasingly shielded upon going from $C_2D_2Cl_4$ to $CDCl_3$. Furthermore, comparison of the ^{1}H NMR spectra of enantiomerically pure *anti*-[Pt(dppp)((+)-**2**)$_2$] and of the mixture of the *syn* and *anti* diastereoisomers of [Pt(dppp)(**2**)$_2$] (Figure S133) shows that the most shielded Me_B protons signals are those of the *anti* diastereoisomer. This observation is a key for the description of the conformation of the copper-free CTB dimers (see Scheme 2).

The formulation [Pt(dppp)(**2**)$_2$CuI] of the complex obtained at high CuI loading was confirmed by reacting [Pt(dppp)(**2**)$_2$], which had been isolated after column chromatography as a 69:31 mixture of *anti*/*syn* diastereoisomers, with a nearly twofold excess of CuI (1.75 equiv) in THF. Comparison of the ^{1}H NMR spectrum of the product with the spectrum of [Pt(dppp)(**2**)$_2$] (Figures S134a and S134b) showed that the diastereoisomeric ratios have been preserved in the course of the reaction as the product had a *d.r.* of 64:36. Comparison with the spectrum of *anti*-[Pt(dppp)((+)-**2**)$_2$CuI] (Figure S134c) confirmed that copper(I) was bound to iodide in this enantiomerically pure complex, and that the most deshielded singlet of the α'_A protons arose from the *anti* diastereoisomer.

To summarize, we have observed that the Me_B protons of *anti*-[Pt(dppp)(**2**)$_2$] were strongly shielded, particularly in $CDCl_3$ (Figure 7), a feature that we also noticed in the case of [Pt(PEt$_3$)$_2$(**2**)$_2$]. This fact could indicate that the Pt-bridged CTB dimers take up a conformation in which the OMe_B substituent of a given CTB is placed in the shielding field of the other CTB in a symmetrical manner. By contrast, the Me_B protons of *syn*-[Pt(dppp)(**2**)$_2$] are less shielded, because only the OMe_B substituent of one CTB can be included in the other CTB. As a

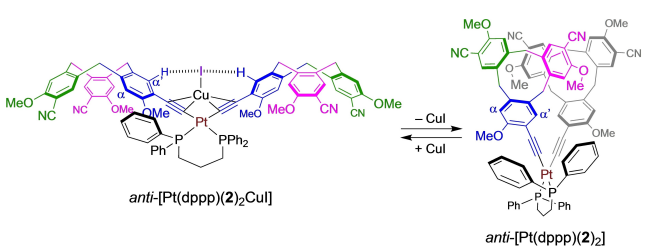

Scheme 2. Illustration, for *anti*-[Pt(dppp)(**2**)$_2$], of the chemical processes taking place at the platinum-bridged CTB dimers and the resulting conformational changes.

Research Article
doi.org/10.1002/ejic.202300284

consequence of the conformational rearrangement of the CTB dimers, the OMe_A substituent is mechanically positioned closer to a phenyl ring of the dppp chelate, which explains the upfield shift of its signals in the ^{1}H NMR spectrum (Figure 7b). This is confirmed by the fact that this feature is not observed in the case of [Pt(PEt_3)$_2$(**2**)$_2$] (Figure S77). The copper(I) complexation/decomplexation processes taking place at the platinum bis-alkynyl chelate, together with the proposed conformational change of the CTB dimer are illustrated in Scheme 2. The conformation of the *anti* diastereoisomers in the copper-free platinum-bridged CTB dimers has some significance, because it makes these complexes resemble chiral molecular tweezers. This family of compounds, first examplified by Whitlock and coll. in 1978[24] covers a wide range of applications, from simple molecular recognition to stimulus-responsive molecular recognition and switching.[25] Therefore, it would be interesting, in the future, to investigate whether these organometallic CTB dimers exhibit molecular tweezers properties.

Detection of "saddle" conformers in both series of complexes

Careful examination by ^{1}H NMR spectroscopy of all the fractions obtained in the course of the chromatographic purification of the *anti*/*syn* diastereoisomeric mixtures of *cis*-[Pt(PEt_3)$_2$(**2**)$_2$] and [Pt(dppp)(**2**)$_2$] allowed us to identify fractions containing products that corresponded neither to the *syn* or the *anti* diastereoisomers characterized so far. In these diastereoisomers, the CTB components display the "cone" conformation, as illustrated in Figure 4. However, CTBs can also exist in the so-called "saddle" conformation, in which one of the aromatic rings is oriented up while the other are oriented down.[2b] Considering again the mixture of the *anti* and *syn* diastereoisomers of *cis*-[Pt(PEt_3)$_2$(**2**)$_2$], examination of the ^{1}H NMR spectra of the different fractions collected in the course of the chromatographic purification of the crude product (Figures S135–S137) showed residual signals in the spectrum of Figure S136 (highlighted in orange), which were predominant in the spectra of the first fractions. Given the fact that they spanned a broad chemical shift range, they could arise from *cis*-[Pt(PEt_3)$_2$(**2**)$_2$] complexes in which the CTBs have indeed the so-called saddle conformation.[2b,26] As a matter of fact, equilibrating a 2:1 *anti*/*syn* diastereoisomeric mixture containing significant amounts of the supposed saddle complexes in $CDCl_3$, led, after 1 day at room temperature followed by heating at 45 °C for 9 h then at 60 °C for 14 h, to a 1:1 *syn*/*anti* ratio together with the decrease of the relative intensities of the signals of the saddle forms (Figure S137).

Furthermore, in the course of the chromatographic purification of the *anti*/*syn* diastereoisomeric mixture of [Pt(dppp)(**2**)$_2$], we realized, also by examination of the different fractions by ^{1}H NMR spectroscopy, that a few of them showed, in addition to the signals of the diastereoisomers, extra signals of lower intensity. Our attention was attracted by the fact that the intensities of these signals increased equally with time when the solutions were abandoned, pointing to the presence of a well-defined, third species in solution (Figure S138). Column chromatography on silicagel allowed us to isolate milligram amounts of the corresponding product, the ^{1}H NMR spectrum of which is shown in Figure S139. This product was isolated in pure form in fractions ahead of those containing *anti*/*syn*-[Pt(dppp)(**2**)$_2$]. Its ESI mass spectrum showed a signal at 1474.43, which corresponded to [{Pt(dppp)(**2**)$_2$}+H$^+$] (Figure S140). In order to further characterize this new isomer of [Pt(dppp)(**2**)$_2$], a sample of contaminated *anti*/*syn*-[Pt(dppp)(**2**)$_2$] was subjected to analytical HPLC on chiral phases using simultaneous UV and polarimetric detection (Figure S141). Chiralpak IH gave four bands peaking at 6.15 (13%), 7.22 (37%), 9.08 (25%), and 9.68 (25%) min. The first and second band had a negative $[\alpha]_D$, the third band did not show any polarimetric response, while the fourth band had a positive $[\alpha]_D$. Chiralpak IG also gave four bands, five in fact, if we take into account the shoulder of the second one, at 6.44 (21%), 7.55 (49%), 9.80 (16%), and 14.78 (14%) min. The first and the third band had a positive $[\alpha]_D$, the second and the fourth, a negative $[\alpha]_D$. Taking into account again the possibility that the CTBs of [Pt(dppp)(**2**)$_2$] can adopt a saddle conformation, five different isomers could be identified from the analytical HPLC experiments (Table S6): The two enantiomers *anti*-(+)-[Pt(dppp)(**2**)$_2$] and *anti*-(−)-[Pt(dppp)(**2**)$_2$],[26] the *meso* diastereoisomer *syn*-[Pt(dppp)(**2**)$_2$], and the two enantiomeric saddle conformers *anti*-(+)-[Pt(dppp)(**2**)(saddle-**2**)], and *anti*-(−)-[Pt(dppp)(**2**)$_2$(saddle-**2**)], in which one CTB is in the saddle conformation, the other being in the cone conformation. Moreover, samples of these isomers could be isolated by preparative HPLC of [Pt(dppp)(**2**)$_2$] (26 mg) on chiral phases. The ECD spectra of the pairs of enantiomers *anti*-(+)-[Pt(dppp)(**2**)$_2$]/*anti*-(−)-[Pt(dppp)(**2**)$_2$] and those of *anti*-(+)-[Pt(dppp)(**2**)(saddle-**2**)]/*anti*-(−)-[Pt(dppp)(**2**)(saddle-**2**)] are reproduced in Figure S142. The latter compounds could be intermediates in the enantiomerization pathway of *anti*-[Pt(dppp)(**2**)$_2$]. For instance, the conversion of [Pt(dppp)((*P*)-**2**)$_2$] into its enantiomer [Pt(dppp)((*M*)-**2**)$_2$] would involve first [Pt(dppp)((*P*)-**2**)(saddle-**2**)] as intermediate for the conversion of [Pt(dppp)((*P*)-**2**)$_2$] into [Pt(dppp)((*P*)-**2**)((*M*)-**2**)], then [Pt(dppp)(saddle-**2**)((*M*)-**2**)] for the conversion of *syn*-[Pt(dppp)(**2**)$_2$] into [Pt(dppp)((*M*)-**2**)$_2$].

We followed the conversion of *anti*-(−)-[Pt(dppp)(**2**)(saddle-**2**)] that was isolated by HPLC into a diastereoisomeric mixture of *anti*- and *syn*-[Pt(dppp)(**2**)$_2$] in cone conformation by ^{1}H NMR spectroscopy in $CDCl_3$ (Figure S143). The conversion was nearly complete after two weeks and produced a *ca.* 1:1 ratio of *anti*- and *syn*-[Pt(dppp)(**2**)$_2$] (Figure S143d). A similar experiment was run in $C_2D_2Cl_4$, in which the rate of conversion was increased by heating at 45 °C (Figure S144).

In summary, the conformational isomerization of the cone form of a CTB component into its saddle form was thus observed in both series of the platinum-bridged CTB dimers. This observation is significant, because it cannot be done in any circumstances. The saddle form of a chiral CTB is the identified intermediate in its enantiomerization pathway. It is less stable than the cone form, and in the case of cyclotriveratrylene the energy difference between the two forms is close to 10 kJmol^{-1}, while the activation energy for the conversion of the cone form into the saddle form is 97.4 kJmol^{-1}.[27] As a consequence, the

Research Article
doi.org/10.1002/ejic.202300284

observation of the saddle form in solutions of cyclotriveratrylene had been unsuccessful until Luz and coworkers discovered an experimental procedure that allowed them to generate and separate it in sizable amounts. However, a cryptophane exhibiting an in-out cone/saddle conformation rather than the classical in-in cone conformation had been isolated earlier and characterized by ^{1}H NMR in solution and X-ray crystallography in the solid state.[28] The in-out cone/saddle conformation was generated by removing an included solvent molecule from a large-size cryptophane. The cryptophane exhibiting this conformation has been called an imploded cryptophane, the cavity being "filled" by one of the twisted phenylene rings of the CTB in saddle conformation. Once dissolved in a solvent, the cryptophane takes back the in-in cone conformation. In the case of the platinum-bridged CTB dimers, the situation is different, unless the interaction of the Me_B substituent of a CTB with the cavity of the other CTB is at the origin of the conformational change.

Attempts to prepare the metallo-cryptophanes from the platinum-bridged dimers

The Pt^{II}-bridged organometallic CTB dimers *anti*-[Pt(dppp)((−)-**1**)$_2$] and [Pt(dppp)(**2**)$_2$], the latter as an *anti*, *syn* diastereoisomeric mixture, were evaluated for their ability to play the role of "pre-cryptophanes", that is, intermediates in the preparation of the organometallic analogues of metallo-cryptophane *anti*-[Pt$_3$(dppp)$_3$(CTB(H,CN)$_2$]$^{6+}$ (Figure 8).[6] First, *anti*-[Pt(dppp)((−)-**1**)$_2$] was combined in CD_2Cl_2 with [Pd(dppp)(OTf)$_2$] in 1:2 molar ratio. The homogeneous reaction mixture was examined by ^{1}H NMR spectroscopy. The spectrum recorded after 24 h did not differ significantly from that after 2 h (Figure S145). Both showed broad features for the CTB component to such an extent that the signals of the α, α′, and γ protons had vanished, while the different axial and equatorial protons were no longer distinguishable, which made their integration underestimated. Less broad were the signals that could be attributed to [Pd(dppp)]$^{2+}$ complex subunits, and the ratio of the aromatic protons to the aliphatic dppp protons was correct, *i.e.*, 78:12 for r-H and 78:6 for s-H. By comparison with their homologs in the precursor *anti*-[Pt(dppp)((−)-**1**)$_2$], the dppp r and s protons were deshielded by ~0.3 ppm, but the r protons were less deshielded than in the case of the metallo-cryptophane *anti*-[Pt$_3$(dppp)$_3$(CTB(H,CN))$_2$](OTf)$_6$.[6a] The ^{31}P NMR spectrum of the reaction mixture after 2 h showed a very broad signal between 16.0 and 14.8 ppm. In another experiment, [Pt(dppp)(**2**)$_2$] in *ca.* 1:1 diastereoisomeric ratio was titrated by [Pt(dppp)(OTf)$_2$]. The experiment was monitored by ^{1}H NMR spectroscopy (10^{-3} molL^{-1} solutions of [Pt(dppp)(**2**)$_2$] in $C_2D_2Cl_4$). A stacked plot of the NMR spectra is displayed in Figure S146. As increasing amounts of [Pt(dppp)(OTf)$_2$] complex subunits were added the signals broadened and their number increased, which was particularly clear in the aromatic region below 7.0 ppm (where the signals of the protons α_A and α'_A, α_B, and α_C are located), and in the region between 4.0 and 3.3 ppm (where the singlets of the methoxy protons are located). The region of the dppp aromatic protons seemed to shrink around prominent signals, and the broad signal of the dppp r protons seemed to disappear at the expense of a less broad signal at ca. 2.75 ppm, close to the chemical shift value of the same protons in [Pt(dppp)(OTf)$_2$]. These features indicated that the [Pt(dppp)]$^{2+}$ indeed reacted with [Pt(dppp)(**2**)$_2$], but did not form a single and well-defined species.

The two-step formation of a metallo-cryptophane via a single platinum-bridged CTB dimer intermediate under kinetic control differs from the one-pot self-assembly of a metallo-cryptophane from its separate components (two equivalents of CTB and three equivalents of bridging metal complex) under thermodynamic control. In the former approach the intramolecular interactions between the CTBs may represent a barrier to the complexation of the two [M(dppp)]$^{2+}$ complex subunits.

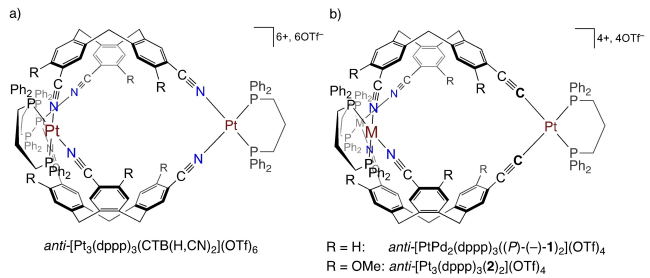

Figure 8. Structures of a) the existing chiral platino-cryptophane based on CTB(H,CN)[6] and of b) the projected isosteric chiral metallo-cryptophanes based on CTBs **1**H and **2**H.

Conclusions

We have reported the preparation of the first cyclotribenzylenes (CTBs) bearing at least two different substituents on the γ′ positions of their large rim. The two asymmetric CTBs **1**H and **2**H were resolved into their enantiomers and their absolute configurations determined. Our objective was to make metallo-cryptophanes incorporating simultaneously inert and labile coordination bonds based respectively on alkynyl and nitrile ligand fragments. The metallo-cryptophane assembly would involve first the preparation of a CTB dimer by formation of a *cis*-platinum(II) bis-alkynyl complex, then the closure of this intermediate by bridging the two pairs of nitrile groups by [ML$_2$]$^{2+}$ complex metal fragments (M = Pd, Pt; L = PEt_3, L_2 = dppp). We prepared the following organometallic platinum dimers from the CTBs and [PtL_2Cl_2] in the presence of substoichiometric amounts of CuI: *cis*-[Pt(PEt_3)$_2$(**1**)$_2$], [Pt(dppp)(**1**)$_2$], *cis*-[Pt(PEt_2)$_2$(**2**)$_2$], and [Pt(dppp)(**2**)$_2$] all in *anti*, *syn* diastereoisomeric mixtures; we also prepared the optically pure complexes [Pt(dppp)((+)-**1**)$_2$], [Pt(dppp)((−)-**1**)$_2$], *cis*-[Pt(PEt_3)$_2$((−)-**2**)$_2$], and [Pt(dppp)((+)-**2**)$_2$], and isolated the pure *syn*-[Pt(dppp)(**2**)$_2$] complex. We observed that, in the case of the complexes of CTB **2**H, the dimers always incorporated either CuI or CuCl, depending on the Cu/Pt ratio. At low CuI loading, CuCl adducts predominated along with copper-free CTB dimers. NMR

spectroscopy studies indicated that the CuX complex fragments were bound in η^2,η^2 fashion to the *cis*-platinum bis(alkynyl) bridging complex fragments, which played the role of pincer complex-as-ligands. Treatment of the binuclear Pt^{II}/Cu^{I} complexes with NaCN allowed us to isolate the copper-free CTB dimers. Reaction of [Pt(dppp)((−)-**1**)$_2$] with two equiv. of [Pd(dppp)(OTf)$_2$] did not afford the sought metallo-cryptophanes, as judged by the ^{1}H NMR analysis. An NMR titration of the *anti*, *syn* mixture of [Pt(dppp)(**2**)$_2$] by [Pt(dppp)(OTf)$_2$] led to the same conclusion. It remains to be tested whether the copper-free CTB dimers in *anti* configuration could be used as ditopic chiral receptors.

Experimental Section

Materials, methods, and instrumentation

The following abbreviations were used: THF (tetrahydrofuran) and DMF (*N*,*N*-dimethylformamide). Unless otherwise stated, all reactions were performed at a vacuum/argon line using Schlenk-type glassware. The following solvents and liquid reagents were dried and distilled under argon prior to use: DMF (anhydrous magnesium sulfate), THF (Na/benzophenone), dichloromethane (P_2O_5), and triethylamine (Na or KOH). Other commercially available solvents and reagents were used as received. Separations by flash column chromatography used either silicagel (Geduran® Si 60, 40–63 μm, from Merck) or aluminum oxide 90 (standardized, according to Brockmann, from Merck). CTB(H,OTf),[6a] CTB(OMe,I),[11] *cis*-[Pt(PEt$_3$)$_2$Cl$_2$],[29] [Pd(dppp)(OTf)$_2$],[30] and [Pt(dppp)Cl$_2$][31] were prepared as reported in the literature. NMR spectra were recorded on Bruker Avance III 400 MHz, 500 MHz and 600 MHz spectrometers. Chemical shifts were reported using the residual solvent ^{1}H signal (7.26 and 77.16 ppm for $CHCl_3$, 5.32 and 54.00 ppm for $CHDCl_2$, 6.00 and 73.78 ppm for C_2DHCl_4) as internal reference for the calibration of the ^{1}H NMR and ^{13}C NMR spectra, respectively, and the phosphorus signal (set at 0 ppm) of a 85% aqueous solution of H_3PO_4 placed inside an insert for the calibration of the ^{31}P NMR spectra. IR spectra were recorded in the ATR mode using a Bruker Alpha II spectrophotometer. ECD spectra and the associated electronic absorption spectra were measured on a JASCO J-815 spectrometer equipped with a JASCO Peltier cell holder PTC-423 to maintain the temperature at 25.0 ± 0.2 °C. A cell of 1 mm of optical pathlength was used. The CD spectrometer was purged with nitrogen before recording each spectrum, which was baseline subtracted. The baseline was always measured for the same solvent and in the same cell as the samples. The spectra were presented without smoothing and further data processing. Optical rotations were measured on a JASCO P-2000 polarimeter with a halogen lamp (589, 578, 546, and 436 nm) in a 10 cm cell thermostated at 25 °C with a Peltier controlled cell holder.

Mass spectrometry experiments. The mass spectrometry data were obtained using a MicrOTOF–Q II (Bruker Daltonics, Bremen, Germany) mass spectrometer fitted with a Z-spray electrospray ion source and operating within a mass range of 2-4000 Thomson. The mass calibration was performed using a mix of Tune Low (Agilent Technologies G1969-8500) prior to analysis. The data were processed with the Data Analysis software from Bruker Daltonics. The mass spectrometer was operated in the positive ion mode, with a potential of 3500 V applied to the electrospray probe body and the source temperature set to 180 °C. Mass spectrometry data were acquired from $m/z = 300$ to 3000. The ISCID energy was kept at 0 eV, while the energy of the collision cell (E_{coll}) was varied from 2 to 20 eV (in some cases up to 200 eV) in order to observe the dissociation of potential dimers. In some specific cases ISCID was varied to increase the intensity of the signal of the molecular peak of interest.

Each sample at a supplied concentration of 10^{-4} mol L^{-1} in $CHCl_3$ or CH_2Cl_2 was diluted to a final concentration of 5×10^{-5} mol L^{-1} with an equal volume of isopropanol containing 1% v/v of formic acid prior to injection into the mass spectrometer.

Theoretical calculations. Molecular structures were optimized at the DFT CAM-B3LYP (with Grimme D3 dispersion corrections) level of theory, using the 6-311 + G(d,p) basis set (Gaussian09 software).[32] Solvent effects were taken into account by PCM model (CH_2Cl_2) and frequency calculations were performed in order to check that true energy minima were obtained. TD-DFT calculations were then performed at the same level of theory.

Compound 3. CTB(H,OTf) (0.300 g; 4.2×10^{-4} mol) and [Pd(PPh$_3$)$_2$Cl$_2$] (0.072 g; 1.02×10^{-4} mol) were dissolved in DMF (15 mL). Triethylamine (2.4 mL; 1.72×10^{-2} mol) was added, followed by a solution of trimethylsilylacetylene (3.2 mL, 0.1 mol L^{-1}; 3.2×10^{-4} mol) in DMF, which was delivered dropwise (20 min). The reaction mixture was heated to 50 °C and stirred at this temperature overnight. After cooling to room temperature, the solvent was removed in vacuo. The crude product was adsorbed on neutral alumina and purified by column chromatography (SiO_2; cyclohexane/dichloromethane 8:2). Pure **3** was isolated as a colorless oil (0.082 g; 30% yield). **3′** (0.005 g), and **3″** (0.005 g) were isolated as side products. **3**: ^{1}H NMR (d^6-acetone; 500.13 MHz, 292.9 K) $\delta = 7.830$ (d, $^3J_{H,H} = 8.5$ Hz, 1 H; α_C-H), 7.798 (d, $^3J_{H,H} = 8.5$ Hz, 1 H; α_B-H), 7.684 (d, $^4J_{H,H} = 2.5$ Hz, 1 H; α'_B-H), 7.663 (d, $^4J_{H,H} = 2.5$ Hz, 1 H; α'_C-H), 7.657 (d, $^4J_{H,H} = 2.5$ Hz, 1 H; α'_A-H), 7.619 (d, $^3J_{H,H} = 8.5$ Hz, 1 H; α_A-H), 7.253 (dd, $^3J_{H,H} = 8.5$ Hz, $^4J_{H,H} = 2.5$ Hz, 1 H; γ_B-H), 7.239 (dd, $^3J_{H,H} = 8.5$ Hz, $^4J_{H,H} = 2.5$ Hz, 1 H; γ_A-H), 7.233 (dd, $^3J_{H,H} = 8.5$ Hz, $^4J_{H,H} = 2.5$ Hz, 1 H; γ_C-H), 5.123 (d, $^2J_{H,H} = 13.5$ Hz, 1 H; a_B-H), 5.109 (d, $^2J_{H,H} = 13.5$ Hz, 1 H; a_C-H), 5.061 (d, $^2J_{H,H} = 13.5$ Hz, 1 H; a_A-H), 5.123 (d, $^2J_{H,H} = 13.5$ Hz, 1 H; a_B-H), 4.032 (d, $^2J_{H,H} = 13.5$ Hz, 1 H; e_B-H), 3.974 (d, $^2J_{H,H} = 13.5$ Hz, 1 H; e_C-H), 3.948 (d, $^2J_{H,H} = 13.5$ Hz, 1 H; e_A-H), 0.201 (s, 9 H; SiCH_3) ppm; ^{13}C NMR (d^6-acetone; 125.77 MHz, 293 K) $\delta = 149.33$ (γ'_C-C), 149.26 (γ'_B-C), 143.31 (β'_C-C), 142.86 (β'_B-C), 141.46 (β_A-C), 140.83 (β_B-C), 140.69 (β_C-C), 140.40 (β'_A-C), 134.24 (α'_A-C), 133.35 (α_C-C), 133.26 (α_B-C), 131.51, 131.46 (α_A-C, γ_A-C), 123.68, 123.66 (α'_B-C, α'_C-C), 122.91 (γ'_A-C), 120.94 (γ_B-C), 120.78 (γ_C-C), 118.33 (CF_3), 105.63 (δ'_A-C), 94.34 (ε'_A-C), 36.81 (CH_2(C)), 36.26 (CH_2(B)), 36.17 (CH_2(A)), 0.25 (SiCH_3) ppm. Elemental analysis: % calcd for $C_{28}H_{24}F_6O_6S_2Si$: C, 50.75; H, 3.65. Found: C, 50.92; H, 3.86.

Compound 1H. A solution of **3** (0.120 g; 1.81×10^{-4} mol) in DMF (5 mL) was transferred into a flask containing solid [Pd(PPh$_3$)$_4$] (0.052 g; 0.45×10^{-5} mol), LiCl (0.046 g; 1.09×10^{-3} mol), and [Zn(CN)$_2$] (0.0859 g; 7.32×10^{-4} mol). The resulting suspension was heated to 120 °C, and stirred at this temperature for 5 days. The solvent was removed under reduced pressure. Chloroform (50 mL) and water (20 mL) were added to the residue, and the resulting mixture sonicated until the organic phase was homogeneous. The aqueous phase was separated and washed with chloroform (2× 15 mL). The combined organic extracts were washed with a saturated aqueous solution of ammonium chloride until a clear organic solution was obtained. After drying ($MgSO_4$) and filtration of the organic phase, the crude product obtained after solvent removal, redissolution in dichloromethane, and adsorption on neutral alumina was purified by column chromatography (SiO_2; cyclohexane/acetone, 75:25). A mixture of three products was obtained, which was applied in the same conditions to a second chromatographic column, affording **1**H (0.037 g) in 59% yield; ^{1}H NMR (d^6-acetone; 500.13 MHz, 293 K) $\delta = 8.008$ (d, $^4J_{H,H} = 1.5$ Hz, 1 H; α'_B-H), 7.982 (d, $^4J_{H,H} = 1.5$ Hz, 1 H; α'_C-H), 7.876 (d, $^3J_{H,H} = 8.0$ Hz, 1 H;

α_C-H), 7.829 (d, $^3J_{H,H}$ = 8.0 Hz, 1 H; α_B-H), 7.700 (d, $^4J_{H,H}$ = 1.5 Hz, 1 H; α'_A-H), 7.666 (d, $^3J_{H,H}$ = 8.0 Hz, 1 H; α_A-H), 7.555 (dd, $^3J_{H,H}$ = 8.0 Hz, $^4J_{H,H}$ = 1.5 Hz, 1 H; γ_B-H), 7.457 (dd, $^3J_{H,H}$ = 8.0 Hz, $^4J_{H,H}$ = 1.5 Hz, 1 H; γ_C-H), 7.283 (dd, $^3J_{H,H}$ = 8.0 Hz, $^4J_{H,H}$ = 1.5 Hz, 1 H; γ_A-H), 5.185 (d, $^2J_{H,H}$ = 13.5 Hz, 1 H; a_B-H), 5.117, 5.110 (d, $^2J_{H,H}$ = 13.5 Hz, 1 H; a_A-H, a_C-H), 4.039 (d, $^2J_{H,H}$ = 13.5 Hz, 1 H; e_B-H), 3.970 (d, $^2J_{H,H}$ = 13.5 Hz, 1 H; e_A-H, e_C-H), 3.629 (s, 1 H; δ'_A-H) ppm; ^{13}C NMR (d^6-acetone; 125.77 MHz, 293 K) δ = 146.12 (β_B-C), 145.32 (β_C-C), 142.01 (β'_C-C), 141.13 (β'_B-C), 140.94 (β_A-C), 139.98 (β'_A-C), 134.84, 134.83 (α'_B-C, α'_C-C), 134.56 (α'_A-C), 132.42 (α_B-C), 132.35 (α_C-C), 131.73 (γ_A-C), 131.59 (α_A-C), 131.57 (γ_C-C), 131.48 (γ_B-C), 122.23 (γ'_A-C), 119.13 (δ'_B-C, δ'_C-C), 111.89 (γ'_C-C), 111.78 (γ'_B-C), 83.78, 79.26 (δ'_A-C, ε'_A-C), 36.82 (*C*H$_2$(A)), 36.63 (*C*H$_2$(B)), 36.54 (*C*H$_2$(C)) ppm. IR (ATR): ν = 3299 (m; C≡**C**–**H**), 2925 (m), 2356 (m), 2227 (s; **C**≡**N**), 2104 (vw, **C**≡**C**), 1734 (m), 1711 (m), 1605 (m), 1565 (m), 1492 (s), 1479 (s), 1401 (m), 1308, 1287, 1243, 1227, 1164, 1154 (w), 1094 (m), 1047 (w), 945 (w), 903 (m), 835 (s), 804 (m), 754 (s), 721 (w), 629, 620 (m), 590 (s), 533 (w), 503 (m) cm^{-1}. LC–MS: *m/z* calcd for $C_{25}H_{16}N_2$, 344.13; found (negative mode), 343.09. Elemental analysis: % calcd for $C_{25}H_{16}N_2$·2 C_3H_6O: C, 80.84; H, 6.13; N, 6.08. Found: C, 80.75; H, 5.67; N, 6.15.

Preparative separation of the enantiomers of 1H by chiral HPLC. A stock solution of (±)-**1**H (*ca.* 0.041 g) was prepared by dissolution in dichloromethane (40 mL). Aliquots of 300 μL were injected every 6.7 minutes into an (*S*,*S*)-Whelk-O1 (250×10 mm) column, eluting with hexane/dichloromethane 35:65 at a flow-rate of 5 mL/min. The fractions collected were detected at 254 nm. The procedure was repeated 132 times affording (+)-**1**H (0.0168 g; >99.5% ee) followed by (−)-**1**H (0.0166 g, >97% ee). Polarimetry of (+)-**1**H: $[\alpha]_{589}^{25}$ = +585 (CH_2Cl_2, *c* = 0.088); polarimetry of (−)-**1**H: $[\alpha]_{589}^{25}$ = −580 (CH_2Cl_2, *c* = 0.086).

Compound 4. CTB(OMe,I) (0.5 g; 0.68 mmol), [Pd(PPh$_3$)$_4$] (0.04 g; 0.034 mmol), and [Zn(CN)$_2$] (0.085 g; 0.72 mmol) were dissolved in DMF (20 mL). The reaction mixture was heated to 120 °C and stirred at this temperature for 2 hr. The solvent was removed in vacuo, and the resulting brown solid subjected to column chromatography (SiO_2, cyclohexane/dichloromethane/ethylacetate from 6:10:0 to 6:10:1.5), which afforded **4** as a colorless solid (0.127 g) in 35% yield, and **4**′ (0.092 g, 21% yield) as side product. **4**: ^{1}H NMR ($CDCl_3$; 500.13 MHz, 292.9 K) δ = 7.734 (s, 1 H; α'_A-H), 7.528 (s, 1 H; α'_C-H), 7.512 (s, 1 H; α'_B-H), 6.902 (s, 1 H; α_B-H), 6.867 (s, 1 H; α_C-H), 6.716 (s, 1 H; α_A-H), 4.733 (d, $^2J_{H,H}$ = 13.5 Hz, 1 H; a_B-H), 4.704 (d, $^2J_{H,H}$ = 13.5 Hz, 1 H; a_A-H), 4.677 (d, $^2J_{H,H}$ = 13.5 Hz, 1 H; a_C-H), 3.938 (s, 3 H; OC*H*$_3$(C)), 3.933 (s, 3 H; OC*H*$_3$(B)), 3.882 (s, 3 H; OC*H*$_3$(A)), 3.687 (d, $^2J_{H,H}$ = 13.5 Hz, 1 H; e_B-H), 3.667 (d, $^2J_{H,H}$ = 13.5 Hz, 1 H; e_A-H), 3.650 (d, $^2J_{H,H}$ = 13.5 Hz, 1 H; e_C-H) ppm; ^{13}C NMR ($CDCl_3$; 125.76 MHz, 293.7 K): δ = 160.30, 160.23 (γ_B-C, γ_C-C), 157.73 (γ_A-C), 146.63 (β_B-C), 145.74 (β_C-C), 140.74 (α'_A-C), 140.35 (β_A-C), 135.23 (α'_C-C), 135.11 (α'_B-C), 131.76 (β'_A-C), 131.63 (β'_C-C), 130.53 (β'_B-C), 116.37 (δ'_B-C, δ'_C-C), 112.82 (α_B-C), 112.62 (α_C-C), 112.14 (α_A-C), 101.09 (γ'_C-C), 100.91 (γ'_B-C), 84.84 (γ'_A-C), 56.74 (OC*H*$_3$(A)), 56.44, 56.38 (OC*H*$_3$(B), OC*H*$_3$(C)), 36.71 (*C*H$_2$(B)), 36.68 (*C*H$_2$(C)), 36.35 (*C*H$_2$(A)) ppm. **4**′: ^{1}H NMR ($CDCl_3$; 500.13 MHz, 295.1 K) δ = 7.736 (s, 1 H; α'_A-H), 7.717 (s, 1 H; α'_B-H), 7.511 (s, 1 H; α'_C-H), 6.885 (s, 1 H; α_C-H), 6.743 (s, 1 H; α_A-H), 6.706 (s, 1 H; α_B-H), 4.720 (d, $^2J_{H,H}$ = 13.5 Hz, 1 H; a_B-H), 4.693 (d, $^2J_{H,H}$ = 13.5 Hz, 1 H; a_C-H), 4.624 (d, $^2J_{H,H}$ = 13.5 Hz, 1 H; a_A-H), 3.922 (s, 3 H; OC*H*$_3$(C)), 3.872 (s, 6 H; OC*H*$_3$(A), OC*H*$_3$(B)), 3.638 (d, $^2J_{H,H}$ = 13.5 Hz, 1 H; e_B-H), 3.621 (d, $^2J_{H,H}$ = 13.5 Hz, 1 H; e_C-H), 3.601 (d, $^2J_{H,H}$ = 13.5 Hz, 1 H; e_A-H) ppm; ^{13}C NMR ($CDCl_3$; 125.77 MHz, 295.1 K): δ = 160.10 (γ_C-C), 157.56, 157.48 (γ_A-C, γ_B-C), 146.50 (β_C-C), 141.10 (β_B-C), 140.76 (α'_A-C), 140.61 (α'_B-C), 140.20 (β_A-C), 135.10 (α'_C-C), 132.97 (β'_A-C), 131.88 (β'_B-C), 131.70 (β'_C-C), 116.53 (δ'_B-C, δ'_C-C), 112.82 (α_C-C), 112.36 (α_B-C), 112.16 (α_A-C), 100.72 (γ'_C-C), 84.71 (γ'_A-C), 84.42 (γ'_B-C), 56.75, 56.70 (OC*H*$_3$(A), OC*H*$_3$(B)), 56.37 (OC*H*$_3$(C)), 36.61 (*C*H$_2$(B)), 36.27 (*C*H$_2$(C)), 36.23 (*C*H$_2$(A)) ppm. Elemental analysis: % calcd for $C_{25}H_{21}I_2NO_3$: C, 47.12; H, 3.32; N, 2.20; found: C, 47.31; H, 3.42; N, 2.50.

Compound 5. **4** (0.085 g; 0.159 mmol), CuI (0.010 g; 0.0525 mmol), and [Pd(PPh$_3$)$_2$Cl$_2$] (0.031 g; 0.0442 mmol) were dissolved in DMF (18 mL). Trimethylsilylacetylene (0.07 mL; 0.492 mmol) and triethylamine (3.0 mL; 21.5 mmol) were added and the reaction mixture heated to 40 °C. After 2 hrs stirring at this temperature, the solvent was removed in vacuo to give a dark-brown residue, which was purified by column chromatography (SiO_2; toluene/ethylacetate, 9:1), which afforded **5** (0.056 g) as a pale yellow solid in 95% yield: MW = 545.73; ^{1}H NMR ($CDCl_3$; 500.13 MHz, 295.1 K) δ = 7.517 (s, 1 H; α'_C-H), 7.507 (s, 1 H; α'_B-H), 7.375 (s, 1 H; α'_A-H), 6.937 (s, 1 H; α_B-H), 6.687 (s, 1 H; α_C-H), 6.751 (s, 1 H; α_A-H), 4.773 (d, $^2J_{H,H}$ = 13.5 Hz, 1 H; a_B-H), 4.703 (d, $^2J_{H,H}$ = 13.5 Hz, 1 H; a_A-H), 4.693 (d, $^2J_{H,H}$ = 13.5 Hz, 1 H; a_C-H), 3.943 (s, 6 H; OC*H*$_3$(B), OC*H*$_3$(C)), 3.877 (s, 3 H; OC*H*$_3$(A)), 3.678 (d, $^2J_{H,H}$ = 13.5 Hz, 1 H; e_B-H), 3.664 (d, $^2J_{H,H}$ = 13.5 Hz, 1 H; e_A-H), 3.651 (d, $^2J_{H,H}$ = 13.5 Hz, 1 H; e_C-H), 0.239 (s, 9 H; Si*CH*$_3$) ppm; ^{13}C NMR ($CDCl_3$; 125.76 MHz, 295.1 K): δ = 160.28, 160.19 (γ_B-C, γ_C-C), 159.71 (γ_A-C), 146.83 (β_B-C), 145.74 (β_C-C), 140.73 (β_A-C), 135.54 (α'_A-C), 135.30 (α'_C-C), 135.06 (α'_B-C), 131.65 (β'_C-C), 130.56 (β'_B-C), 129.48 (β'_A-C), 116.43 (δ'_B-C, δ'_C-C), 113.03 (α_B-C), 112.61 (α_C-C), 112.20 (α_A-C), 112.09 (γ'_A-C), 101.06 (γ'_C-C), 100.83 (γ'_B-C), 100.69 (δ'_A-C), 99.02 (ε'_A-C), 56.43, 56.37, 56.34 (OC*H*$_3$(A), OC*H*$_3$(B), OC*H*$_3$(C)), 36.91 (*C*H$_2$(A)), 36.75 (*C*H$_2$(B)), 36.60 (*C*H$_2$(C)), 0.21 (Si*C*H$_3$) ppm. Elemental analysis: % calcd for $C_{31}H_{30}N_2O_3Si$·2/3H_2O: C, 71.79; H, 6.09; N, 5.40; found: C, 71.76; H, 5.88; N. 5.35.

Compound 2H. To a solution of **5** (0.048 g, 0.095 mmol) in THF (4 mL) was added a solution of tetrabutylammonium fluoride in THF (0.5 mL of a 1 M solution; 0.5 mmol). The reaction mixture was stirred at room temperature for 4 hrs. The solvent was removed in vacuo and the residue soaked in water (50 mL). The resulting mixture was extracted into dichloromethane (3×25 mL). The organic phase was washed with water, dried ($MgSO_4$), filtered, and the solvent evaporated under vacuum to afford **2**H (0.040 g) in 97% yield: ^{1}H NMR ($CDCl_3$; 500.13 MHz, 295.1 K) δ = 7.535 (s, 1 H; α'_C-H), 7.513 (s, 1 H; α'_B-H), 7.421 (s, 1 H; α'_A-H), 6.934 (s, 1 H; α_B-H), 6.874 (s, 1 H; α_C-H), 6.797 (s, 1 H; α_A-H), 4.787 (d, $^2J_{H,H}$ = 13.5 Hz, 1 H; a_B-H), 4.728 (d, $^2J_{H,H}$ = 13.5 Hz, 1 H; a_C-H), 4.719 (d, $^2J_{H,H}$ = 13.5 Hz, 1 H; a_A-H), 3.941 (s, 3 H; OC*H*$_3$(C)), 3.934 (s, 3 H; OC*H*$_3$(B)), 3.912 (s, 3 H; OC*H*$_3$(A)), 3.693 (d, $^2J_{H,H}$ = 13.5 Hz, 1 H; e_B-H), 3.680 (d, $^2J_{H,H}$ = 13.5 Hz, 1 H; e_A-H), 3.677 (d, $^2J_{H,H}$ = 13.5 Hz, 1 H; e_C-H), 3.272 (s, 1 H; δ'_A-H) ppm; ^{1}H NMR (CD_2Cl_2; 500.13 MHz, 298 K) δ = 7.570 (s, 1 H; α'_C-H), 7.558 (s, 1 H; α'_B-H), 7.449 (s, 1 H; α'_A-H), 6.964 (s, 1 H; α_B-H), 6.924 (s, 1 H; α_C-H), 6.830 (s, 1 H; α_A-H), 4.804 (d, $^2J_{H,H}$ = 13.5 Hz, 1 H; a_B-H), 4.751 (d, $^2J_{H,H}$ = 13.5 Hz, 1 H; a_C-H), 4.743 (d, $^2J_{H,H}$ = 13.5 Hz, 1 H; a_A-H), 3.939 (s, 3 H; OC*H*$_3$(C)), 3.934 (s, 3 H; OC*H*$_3$(B)), 3.878 (s, 3 H; OC*H*$_3$(A)), 3.716 (d, $^2J_{H,H}$ = 13.5 Hz, 1 H; e_B-H), 3.703 (d, $^2J_{H,H}$ = 13.5 Hz, 1 H; e_A-H), 3.694 (d, $^2J_{H,H}$ = 13.5 Hz, 1 H; e_C-H), 3.268 (s, 1 H; δ'_A-H) ppm; ^{13}C NMR ($CDCl_3$; 125.76 MHz, 295.1 K): δ = 160.32 (γ_B-C), 160.25 (γ_C-C), 159.95 (γ_A-C), 146.70 (β_B-C), 145.79 (β_C-C), 141.15 (β_A-C), 135.61 (α'_A-C), 135.31 (α'_C-C), 135.10 (α'_B-C), 131.51 (β'_C-C), 130.56 (β'_B-C), 129.66 (β'_A-C), 116.39 (δ'_B-C, δ'_C-C), 112.93 (α_B-C), 112.64 (α_C-C), 112.07 (α_A-C), 110.89 (γ'_A-C), 101.12 (γ'_C-C), 100.91 (γ'_B-C), 81.48, 79.59 (δ'_A-C, ε'_A-C), 56.43, 56.39, 56.32 (OC*H*$_3$(A), OC*H*$_3$(B), OC*H*$_3$(C)), 36.92 (*C*H$_2$(A)), 36.76 (*C*H$_2$(B)), 36.61 (*C*H$_2$(C)) ppm. IR (ATR): ν = 3282 (m; C≡**C**–**H**), 2932, 2920 (w), 2850 (vw), 2224 (s; **C**≡**N**), 2103 (vw, **C**≡**C**), 1980 (vw), 1606 (s), 1567 (m), 1499 (vs), 1476 (s), 1460, 1444, 1392, 1312, 1270 (vs), 1209 (s), 1181, 1141 (m), 1079 (vs), 1003 (s), 940, 927 (m), 896 (w), 853, 835 (m), 797 (vw), 739 (s), 679, 643 (m), 607 (s), 533, 510, 467 (m), 428 (w) cm^{-1}. Elemental analysis: % calcd for $C_{28}H_{22}N_2O_3$·1/3CH_2Cl_2·2/3H_2O: C, 72.59; H, 5.02; N, 5.98; found: C, 72.77; H, 4.98; N. 6.03.

Preparative separation of the enantiomers of 2H by chiral HPLC. A stock solution of (±)-**2**H (*ca.* 0.057 g) was prepared by dissolution in dichloromethane (65 mL). Aliquots of 800 μL were injected every

6 minutes into an (*S,S*)-Whelk-O1 (250×10 mm) column, eluting with hexane/ethanol/dichloromethane 30:10:60 at a flow-rate of 5 mL/min. The fractions collected were detected at 254 nm. The procedure was repeated 82 times affording (+)-**2**H (0.0178 g, >98% ee) followed by (−)-**2**H (0.0185 g; >99% ee). Polarimetry of (+)-**2**H: $[\alpha]_{589}^{25} = +6$ (CH_2Cl_2, $c = 0.06$); polarimetry of (−)-**2**H: $[\alpha]_{589}^{25} = -6$ (CH_2Cl_2, $c = 0.07$).

***anti*-[Pt(dppp)((−)-(1)$_2$]**. (−)-**1**H (0.007 g; 0.0203 mmol), [Pt-(dppp)Cl_2] (0.0051 g; 0.0075 mmol), CuI (0.001 g; 0.00525 mmol), and triethylamine (0.05 mL; 0.359 mmol) were mixed in THF (5 mL). The reaction mixture was stirred for 24 hrs at room temperature. After TLC control, which indicated that significant amounts of starting CTB were still present, additional portions of [Pt(dppp)Cl_2] (0.0025 g; 0.0037 mmol), CuI (0.001 g; 0.00525 mmol), and triethylamine (0.02 mL; 0.144 mmol) were added. The reaction was stirred for 3 days more. The solvent was removed under vacuum and the residue taken up in water (30 mL). The product was extracted into dichloromethane (10 mL). After addition of an aqueous solution of sodium hydroxide (1 M; 10 mL), the aqueous phase was further extracted with dichloromethane (2×10 mL). The organic phase was concentrated by rotary evaporation. The residue, after adsorption on neutral alumina, was submitted to column chromatography (SiO_2; cyclohexane/acetone 6:4), which afforded *anti*-[Pt(dppp)((−)-**1**)$_2$] (0.0071 g) as a pure product in 54% yield; ^{1}H NMR (CD_2Cl_2; 500.13 MHz, 295 K): $\delta = 7.763$ (br dd, 4 H; o-H), 7.727 (br dd, 4 H; o′-H), 7.627 (d, $^4J_{H,H} = 1.5$ Hz, 2 H; α'_B-H), 7.611 (d, $^4J_{H,H} = 1.5$ Hz, 2 H; α'_C-H), 7.456 (d, $^3J_{H,H} = 8.0$ Hz, 2 H; α_C-H), 7.426, 7.409 (2 t, $^3J_{H,H} = 8.0$ Hz, 2×2 H; p-H, p′-H), 7.396 (dd, $^3J_{H,H} = 8.0$ Hz, $^4J_{H,H} = 1.5$ Hz, 2 H; γ_C-H), 7.377–7.345 (d, $^3J_{H,H} = 8.0$ Hz, 8 H; m-H, m′-H), 7.353 (d, $^3J_{H,H} = 8.0$ Hz, 2 H; α_B-H), 7.318 (dd, $^3J_{H,H} = 8.0$ Hz, $^4J_{H,H} = 1.5$ Hz, 2 H; γ_B-H), 7.040 (d, $^3J_{H,H} = 8.0$ Hz, 2 H; α_A-H), 6.915 (d, $^4J_{H,H} = 1.5$ Hz, 2 H; α'_A-H), 6.459 (dd, $^3J_{H,H} = 8.0$ Hz, $^4J_{H,H} = 1.5$ Hz, 2 H; γ_A-H), 4.900 (d, $^2J_{H,H} = 13.5$ Hz, 2 H; a_B-H), 4.732 (d, $^2J_{H,H} = 13.5$ Hz, 2 H; a_C-H), 4.727 (d, $^2J_{H,H} = 13.5$ Hz, 2 H; a_A-H), 3.778 ($^2J_{H,H} = 13.5$ Hz, 2 H; e_B-H), 3.677 (d, $^2J_{H,H} = 13.5$ Hz, 2 H; e_C-H), 3.613 (d, $^2J_{H,H} = 13.5$ Hz, 2 H; e_A-H), 2.494 (quint., 4 H; r-H), 2.029 (m, 2 H; s-H) ppm; ^{13}C NMR (CD_2Cl_2; 125.76 MHz, 295 K): $\delta =$ 145.59 (β_B-C), 144.09 (β_C-C), 141.58 (β'_C-C), 139.81 (β'_B-C), 137.72 (β'_A-C), 135.82 (β_A-C), 134.30, 134.26 (2 d, $^2J_{C,P} = 5.3$ Hz; o1-C, o2-C), 134.21 (α'_B-C), 134.00, 133.95 (2 d, $^2J_{C,P} = 5.3$ Hz; o′1-C, o′2-C), 133.06 (α'_A-C), 131.88 (ε'_A-C, α_B-C), 131.40 (α_C-C), 131.22 (γ_C-C or γ_B-C), 131.18 (p-C), 131.08 (p′-C, γ_C-C or γ_B-C), 130.93 (γ_A-C), 129.92 (α_A-C), 128.86, 128.81 (2 d, $^3J_{C,P} = 5.2$ Hz; m-C, m′-C), 127.80 (γ'_A-C), 119.15, 119.13 (δ'_B-C, δ'_C-C), 111.72 (γ'_C-C), 111.36 (γ'_B-C), 109.58 (δ'_A-C), 37.36 (CH_{2A}), 37.09 (CH_{2B}), 36.93 (CH_{2C}), 26.62 (t, $^2J_{C,P} = 18$ Hz; r-C), 20.71 (s-C) ppm; $[\alpha]_{589}^{25} = +340$ (CH_2Cl_2, $c = 0.046$); ESI-MS: m/z calcd for $C_{77}H_{56}N_4NaP_2Pt$, 1316.35256; found 1316.33 for $[M+Na]^+$.

***cis*-[(Pt(PEt$_3$)$_2$(2)$_2$)CuCl]**. A mixture of **2**H (0.105 g; 0.242 mmol), *cis*-[Pt(PEt_3)$_2Cl_2$] (0.0705 g; 0.140 mmol), CuI (0.012 g; 0.630 mmol), triethylamine (1.0 mL; 7.17 mmol) in THF (25 mL) was stirred at room temperature for 2 days. The solvent was removed under vacuum and the residue purified by column chromatography (SiO_2; cyclohexane/dichloromethane/ethylacetate from 6:10:1 to 6:10:6 v/v), which afforded *cis*-[(Pt(PEt_3)$_2$(**2**)$_2$CuCl] (0.0844 g; 0.0604 mmol) in 50% yield and 66:34 *anti/syn* diastereoisomeric ratio. ^{1}H NMR (CD_2Cl_2; 600.13 MHz, 298 K): $\delta = 8.524$ (s, 2 H; α'_A-H, *anti*), 8.407 (s, 2 H; α'_A-H, *syn*), 7.562 (s, 2 H; α'_C-H, *syn*), 7.554 (s, 2 H; α'_C-H, *anti*), 7.493 (s, 2 H; α'_B-H, *syn*), 7.400 (br s, 2 H; α'_B-H, *anti*), 7.389 (s, 2 H; α_B-H, *anti*), 7.317 (s, 2 H; α_B-H, *syn*), 6.912 (s, 2 H; α_C-H, *syn*), 6.844 (br s, 2 H; α_C-H, *anti*), 6.722 (s, 2 H; α_A-H, *syn*), 6.679 (s, 2 H; α_A-H, *anti*), 4.817 (d, $^2J_{H,H} = 13.5$ Hz, 2 H; a_C-H, *syn*), 4.733 (d, $^2J_{H,H} = 13.5$ Hz, 2 H; a_A-H, *syn*), 4.725 (d, $^2J_{H,H} = 13.5$ Hz, 2 H; a_A-H, *anti*), 4.702 (d, $^2J_{H,H} =$ 13.5 Hz, 2×2 H; a_B-H, *syn*, a_C-H, *anti*), 4.681 (d, $^2J_{H,H} = 13.5$ Hz, 2 H; a_B-H, *anti*), 4.008 (s, 6 H; OCH_{3B}, *anti*), 3.942 (s, 6 H; OCH_{3C}, *anti*), 3.932 (s, 6 H; OCH_{3C}, *syn*), 3.909 (s, 6 H; OCH_{3B}, *syn*), 3.828 (s, 6 H; OCH_{3A}, *syn*), 3.796 (d, $^2J_{H,H} = 13.5$ Hz, 2 H; e_B-H, *syn*), 3.773 (d, $^2J_{H,H} = 13.5$ Hz, 8 H; e_B-H, *anti*, OCH_{3A}, *anti*), 3.688 (d, $^2J_{H,H} = 13.5$ Hz, 2 H; e_A-H, *anti*), 3.681 (d, $^2J_{H,H} = 13.5$ Hz, 2 H; e_C-H, *syn*), 3.654 (d, $^2J_{H,H} = 13.5$ Hz, 2 H; e_A-H, *syn*), 3.518 (br d, $^2J_{H,H} = 13.5$ Hz, 2 H; e_C-H, *syn*), 2.035 (m, 2×12 H; P$CH_2$$CH_3$, *anti* and *syn*), 1.119 (m, 18 H; PCH_2CH_3, *anti*), 1.116 (m, 18 H; PCH_2CH_3, *syn*) ppm; ^{31}P NMR (CD_2Cl_2; 121.49 MHz, 298 K): $\delta =$ 4.18 (*anti*), 4.23 (*syn*) ppm ($^1J_{P,Pt} = 2495$ Hz); ESI-MS: *m/z* calcd for $C_{68}H_{72}CuN_4O_6P_2Pt$, 1360.38708; found, 1360.36 (80%) for $[M+Cu]^+$; *m/z* calcd for $C_{68}H_{72}N_4NaO_6P_2Pt$, 1320.44725; found 1320.44 (7.7%) for $[M+Na]^+$.

[Pt(dppp)(2)$_2$CuCl] and [Pt(dppp)(2)$_2$CuI]. **2**H (0.040 g; 0.0921 mmol), [Pt(dppp)Cl_2] (0.0374 g; 0.0551 mmol), copper iodide (0.00528 g; 0.02772 mmol), and triethylamine (0.33 mL; 2.3676 mmol) were mixed in THF (15 mL). The reaction mixture was stirred at room temperature for 4 days. The solvent was removed by rotary evaporation and the residue purified by column chromatography (SiO_2; cyclohexane/dichloromethane/ethylacetate from 3:5:0.5 to 3:5:2, v/v), which afforded first [Pt(dppp)(**2**)$_2$CuI] (0.008 g; 0.04805 mmol) as a mixture of diastereoisomers in *ca.* 1:0.95 *anti/syn* ratio and 10% yield, then [Pt(dppp)(**2**)$_2$CuCl] (0.020 g; 0.01271 mmol) as a mixture of diastereoisomers in 28% yield and 1:0.62 *anti/syn* ratio. ^{1}H NMR spectra reproduced in Figure S109. Elemental analyses: [Pt(dppp)(**2**)$_2$CuCl]·2 C_6H_{12}, % calcd for $C_{95}H_{92}CuClN_4O_6P_2Pt$: C, 65.51; H, 5.32; N, 3.22; found: C, 65.96; H, 5.34; N. 3.43; [Pt(dppp)(**2**)$_2$CuI]·3/2CH_2Cl_2: C, 56.63; H, 3.99; N, 3.13; found: 56.35; H, 4.02; N, 3.31.

***anti*-[Pt(dppp)((+)-2)$_2$CuI]**. (+)-**2**H (0.0165 g; 0.0380 mmol), [Pt-(dppp)Cl_2] (0.0143 g; 0.02108 mmol), copper iodide (0.0035 g; 0.0184 mmol), and triethylamine (0.550 mL; 3.946 mmol) were mixed in THF (11 mL). The reaction mixture was stirred at room temperature for 6 hrs. The solvent was removed by rotary evaporation, and the residue was purified by column chromatography (SiO_2; cyclohexane/acetone 4:3 then 1:1, v/v), which afforded first [Pt(dppp)((+)-**2**)$_2$] (0.005 g; 0.00339 mmol) in 18% yield, then [Pt(dppp)((+)-**2**)$_2$CuI] (0.012 g; 0.00721 mmol) in 38% yield. A 7.5 mg sample of the latter was further purified by HPLC on Chiralpak ID (250×4.6 mm), eluting with hexane/ethanol/CH_2Cl_2 50:10:40 at a flow rate of 1 mL mn^{-1}. 26 injections of 50 µL each afforded 3.1 mg of *anti*-[Pt(dppp)((+)-**2**)$_2$CuI], $[\alpha]_{589}^{25} = +202$ (CH_2Cl_2, $c = 0.16$); ^{1}H NMR ($CDCl_3$; 500.13 MHz, 295.1 K): $\delta = 8.261$ (s, 2 H; α'_A-H), 7.737 (br t, 4 H; o-H), 7.656 (t, 4 H; o′-H), 7.446 (s, 2 H; α'_C-H), 7.435 (s, 2 H; α'_B-H), 7.374 (br t, 4 H; p-H), 7.310 (br t, 4 H; m-H), 7.235 (s, 2 H; α_B-H), 7.118 (br t, 4 H; m′-H), 7.088 (br t, 2 H; p′-H), 6.847 (s, 2 H; α_C-H), 6.415 (s, 2 H; α_A-H), 4.751 (d, $^2J_{H,H} = 13.5$ Hz, 2 H; a_C-H), 4.622 (d, $^2J_{H,H} = 13.5$ Hz, 2 H; a_A-H), 4.563 (d, $^2J_{H,H} = 13.5$ Hz, 2 H; a_B-H), 3.927 (s, 6 H; OCH_{3C}), 3.867 (s, 6 H; OCH_{3B}), 3.728 (d, $^2J_{H,H} =$ 13.5 Hz, 2 H; e_B-H), 3.608 (d, $^2J_{H,H} = 13.5$ Hz, 2 H; e_C-H), 3.536 (d, $^2J_{H,H} = 13.5$ Hz, 2 H; e_A-H), 3.502 (s, 6 H, OCH_{3A}), 2.478 (br m, 4 H; r-H), 2.075 (br m, 2 H; s-H) ppm; ^{13}C NMR ($CDCl_3$; 125.76 MHz, 295 K): $\delta =$ 160.52 (γ_B-C), 160.00 (γ_C-C), 158.68 (γ_A-C), 147.72 (β_B-C), 146.13 (β_C-C), 138.57 (β_A-C), 135.28 (α'_C-C), 135.22 (α'_A-C), 134.49 (α'_B-C), 133.83 (br t; o-C), 133.44 (br t; o′-C), 132.31 (β'_C-C), 131.15 (br s; p′-C), 130.98 (br s; p-C), 130.12 (β'_B-C), 128.72 (β'_A-C), 128.59 (br t; m-C), 128.44 (m′-C), 116.90, 116.67 (δ'_B-C and δ'_C-C), 114.20 (α_B-C), 113.63 (γ'_A-C), 112.59 (α_C-C), 110.53 (α_A-C), 100.62 (γ'_C-C), 99.96 (γ'_B-C), 58.11 (OCH_{3B}), 56.40 (OCH_{3C}), 55.09 (OCH_{3A}), 36.72 (CH_{2C}), 36.50 (br s; CH_{2A} and CH_{2B}), 25.82 (vw s; r-C), 20.01 (vw s, s-C) ppm; ^{31}P NMR (CD_2Cl_2; 202.50 MHz, 298 K): $\delta = 4.21$ ($^1J_{P,Pt} = 2500$ Hz) ppm; ESI-MS: *m/z* calcd for $C_{83}H_{68}N_4NaO_6P_2Pt$, 1496.41595; found, 1496.42 (100%) for $[M–Cu+Na]^+$; *m/z* calcd for $C_{83}H_{68}CuN_4O_6P_2Pt$, 1536.35578; found, 1536.36 (42%) for $[M]^+$.

***syn*-[Pt(dppp)(2)$_2$CuCl] and *anti*-[Pt(dppp)(2)$_2$CuCl]**. **2**H (0.020 g; 0.0460 mmol), [Pt(dppp)Cl_2] (0.0241 g; 0.0355 mmol), copper iodide (0.002 g; 0.010 mmol), and triethylamine (0.300 mL; 2.15 mmol) were mixed in THF (7 mL). The reaction mixture was stirred at room temperature for 6 hrs. The solvent was removed by rotary

Research Article
doi.org/10.1002/ejic.202300284

evaporation. The residue was retaken in dichloromethane (30 mL) and the solution was washed with water (3×20 mL), dried ($MgSO_4$), and evaporated to dryness. The crude product was first isolated by precipitation from dichloromethane/cyclohexane. It was further purified by chromatography (SiO_2; cyclohexane/CH_2Cl_2/ethylacetate 3:5:3) to afford [Pt(dppp)(**2**)$_2$CuCl] (0.009 g, 5.72 10^{-3} mmol) in 25% yield as a mixture of *syn* and *anti* diastereoisomers. The product was examined by analytical chiral HPLC using a Chiralpak IE column and eluting with heptane/ethanol/dichloromethane 40:20:40 at a flow rate of 1 mL min^{-1}. The chromatogram showed three bands at 6.99, 8.67, and 10.42 min, the first ones corresponding to the enantiomers of the chiral form and the last one to the *meso* diastereoisomer, as indicated by the CD at 254 nm. Preparative HPLC in the same conditions allowed us to separate the *meso* form, *syn*-[Pt(dppp)(**2**)$_2$CuCl] (0.0025 g) from the mixture of enantiomers, *anti*-[Pt(dppp)(**2**)$_2$CuCl] (0.0045 g), but the resolution of the latter turned out not to be possible in these conditions. ^{1}H NMR spectra of the separated diastereoisomers are shown in Figure S108.

***anti*-[Pt(dppp)((+)-2)$_2$]**. *anti*-[Pt(dppp)((+)-**2**)$_2$CuI] (0.003 g; 0.186×10^{-5} mol) was dissolved in CH_2Cl_2 (2 mL) and stirred with a solution of NaCN (0.0015 g; 3.061×10^{-5} mol) in water (1 mL) at 0 °C for 2 hrs. The organic phase was separated, evaporated to dryness at 0 °C and further dried under vacuum to afford the enantiomerically-pure *anti*-[Pt(dppp)((+)-**2**)$_2$]. The ^{1}H NMR spectra in three different solvents ($CDCl_3$, CD_2Cl_2, and $C_2D_2Cl_4$) are shown in Figure S132.

Separation of the different conformers of [Pt(dppp)(2)$_2$] by HPLC on chiral phases

The first run, conducted with Chiralpak IH afforded pure *anti*-(−)-[Pt(dppp)(**2**)(saddle-**2**)] (1.8 mg), a mixture of *anti*-(+)-[Pt(dppp)(**2**)(saddle-**2**)] and *anti*-(−)-[Pt(dppp)(**2**)$_2$], pure *syn*-[Pt(dppp)(**2**)$_2$] (2.5 mg), and a mixture of *syn*-[Pt(dppp)(**2**)$_2$] and *anti*-(+)-[Pt(dppp)(**2**)$_2$]. The mixture of *anti*-(+)-[Pt(dppp)(**2**)(saddle-**2**)] and *anti*-(−)-[Pt(dppp)(**2**)(saddle-**2**)] was separated on a Chiralpak IA column, which afforded pure *anti*-(+)-[Pt(dppp)(**2**)(saddle-**2**)] (1.2 mg) and pure *anti*-(−)-[Pt(dppp)(**2**)$_2$]; the mixture of *syn*-[Pt(dppp)(**2**)$_2$] and *anti*-(+)-[Pt(dppp)(**2**)$_2$] was separated on a Chiral Art Cellulose SJ, which afforded pure *anti*-(+)-[Pt(dppp)(**2**)$_2$] (3 mg) and pure *syn*-[Pt(dppp)(**2**)$_2$] (1.6 mg; intermediate fractions represented a total of 11.5 mg and consisted of mixtures of isomers). The ECD spectra of the pairs of enantiomers *anti*-(+)-[Pt(dppp)(**2**)$_2$]/*anti*-(−)-[Pt(dppp)(**2**)$_2$] and those of *anti*-(+)-[Pt(dppp)(**2**)(saddle-**2**)]/*anti*-(−)-[Pt(dppp)(**2**)(saddle-**2**)] are reproduced in Figure S142a.

Acknowledgements

We thank the French National Research Agency (ANR) through the "Programme d'Investissement d'Avenir" under contract 17-EURE-0016 (PhD fellowship to JZ), the CNRS and the University of Strasbourg for financial support. The EXPLOR mesocenter is thanked for providing access to their computing facility (project 2021CPMXX2483). We are grateful to one of the referees for pertinent and helpful observations.

Conflict of Interests

The authors declare no conflict of interest.

Data Availability Statement

The data that support the findings of this study are available in the supplementary material of this article.

Keywords: alkyne ligands · chirality · copper · cyclophanes · platinum

[1] a) J. J. Henkelis, M. J. Hardie, *Chem. Commun.* **2015**, *51*, 11929; b) N. J. Cookson, J. M. Fowler, D. P. Martin, J. Fisher, J. J. Henkelis, T. K. Ronson, F. L. Thorp-Greenwood, C. E. Willans, M. J. Hardie, *Supramol. Chem.* **2018**, *30*, 255.
[2] a) J. Gabard, A. Collet, *J. Chem. Soc., Chem. Commun.* **1981**, 1137; b) A. Collet, *Tetrahedron* **1987**, *43*, 5725; c) A. Collet, J.-P. Dutasta, B. Lozach, J. Canceill, *Top. Curr. Chem.* **1993**, *165*, 103; d) T. Brotin, J.-P. Dutasta, *Chem. Rev.* **2009**, *109*, 88; e) G. El-Ayle, K. T. Holman in *Comprehensive Supramolecular Chemistry II* (Ed.: J. L. Atwood), **2017**, pp. 199–249.
[3] a) M. M. Spence, E. J. Ruiz, S. M. Rubin, T. J. Lowery, N. Wissinger, P. G. Schultz, D. E. Wemmer, A. Pines, *J. Am. Chem. Soc.* **2004**, *126*, 15287; b) P. Berthault, G. Huber, H. Desvaux, *Prog. Nucl. Magn. Reson. Spectrosc.* **2009**, *55*, 35; c) J. Sloniec, M. Schnurr, C. Witte, U. Resch-Genger, L. Schröder, A. Hennig, *Chem. Eur. J.* **2013**, *19*, 3110; d) S. Klippel, J. Döpfert, J. Jayapaul, M. Kunth, F. Rossella, M. Schnurr, C. Witte, C. Freund, L. Schröder, *Angew. Chem. Int. Ed.* **2014**, *53*, 493; e) T. Brotin, E. Jeanneau, P. Berthault, E. Léonce, D. Pitrat, J.-C. Mulatier, *J. Org. Chem.* **2018**, *83*, 14465; f) E. Léonce, T. Brotin, P. Berthault, *Phys. Chem. Chem. Phys.* **2022**, *24*, 24793.
[4] a) J. A. Wytko, J. Weiss, *Tetrahedron Lett.* **1991**, *32*, 7261; b) J. A. Wytko, J. Weiss, *J. Inclusion Phenom. Mol. Recognit. Chem.* **1994**, *19*, 207; c) Z. Zhong, A. Ikeda, S. Shinkai, S. Sakamoto, K. Yamaguchi, *Org. Lett.* **2001**, *3*, 1085; d) J. J. Henkelis, C. J. Carruthers, S. E. Chambers, R. Clowes, A. I. Cooper, J. Fisher, M. J. Hardie, *J. Am. Chem. Soc.* **2014**, *136*, 14393; e) V. E. Pritchard, D. Rota Martir, S. Oldknow, S. Kai, S. Hiraoka, N. J. Cookson, E. Zysman-Colman, M. J. Hardie, *Chem. Eur. J.* **2017**, *23*, 6290; f) T. Kojima, F. L. Thorp-Greenwood, M. J. Hardie, S. Hiraoka, *Chem. Sci.* **2018**, *9*, 4104; g) S. Oldknow, D. Rota Martir, V. E. Pritchard, M. A. Blitz, C. W. G. Fishwick, E. Zysman-Colman, M. J. Hardie, *Chem. Sci.* **2018**, *9*, 8150; h) E. Britton, R. J. Ansell, M. J. Howard, M. J. Hardie, *Inorg. Chem.* **2021**, *60*, 12912.
[5] T. K. Ronson, H. Nowell, A. Westcott, M. J. Hardie, *Chem. Commun.* **2011**, *47*, 176.
[6] a) A. Schaly, Y. Rousselin, J.-C. Chambron, E. Aubert, E. Espinosa, *Eur. J. Inorg. Chem.* **2016**, 832; b) A. Schaly, M. Meyer, J.-C. Chambron, M. Jean, N. Vanthuyne, E. Aubert, E. Espinosa, N. Zorn, E. Leize-Wagner, *Eur. J. Inorg. Chem.* **2019**, 2691.
[7] N. Kotera, L. Delacour, T. Traoré, N. Tassali, P. Berthault, D.-A. Buisson, J.-P. Dognon, B. Rousseau, *Org. Lett.* **2011**, *13*, 2153.
[8] a) M. Hissler, W. B. Connick, D. K. Geiger, J. E. McGarrah, D. Lipa, R. J. Lachicotte, R. Eisenberg, *Inorg. Chem.* **2000**, *39*, 447; b) S.-C. Chan, M. C. W. Chan, Y. Wang, C.-M. Che, K.-K. Cheung, N. Zhu, *Chem. Eur. J.* **2001**, *7*, 4180; c) U. Siemeling, K. Bausch, H. Fink, C. Bruhn, M. Baldus, B. Angerstein, R. Plessow, A. Brockhinke, *Dalton Trans.* **2005**, 2365; d) C. J. Adams, N. Fey, Z. A. Harrison, I. V. Sazanovich, M. Towrie, J. A. Weinstein, *Inorg. Chem.* **2008**, *47*, 8242.
[9] C. M. Álvarez, L. A. García-Escudero, R. García-Rodríguez, J. M. Martín-Álvarez, D. Miguel, V. M. Rayón, *Dalton Trans.* **2014**, *43*, 15693.
[10] a) J. A. Whiteford, C. V. Lu, P. J. Stang, *J. Am. Chem. Soc.* **1997**, *119*, 2524; b) J. A. Whiteford, P. J. Stang, S. D. Huang, *Inorg. Chem.* **1998**, *37*, 5595; c) C. Müller, J. A. Whiteford, P. J. Stang, *J. Am. Chem. Soc.* **1998**, *120*, 9827; d) H. Jiang, A. Hu, W. Lin, *Chem. Commun.* **2003**, 96; e) Y. Ai, M. Ng, E. Y.-H. Hong, A. K.-W. Chan, Z.-W. Wei, Y. Li, V. W.-W. Yam, *Chem. Eur. J.* **2018**, *24*, 11611.
[11] L. Peyrard, S. Chierici, S. Pinet, P. Batat, G. Jonusauskas, N. Pinaud, P. Meyrand, I. Gosse, *Org. Biomol. Chem.* **2011**, *9*, 8489.
[12] a) M. Alami, F. Ferri, G. Linstrumelle, *Tetrahedron Lett.* **1993**, *34*, 6403; b) N. E. Leadbeater, B. J. Tominack, *Tetrahedron Lett.* **2003**, *44*, 8653.
[13] a) H. G. Selnick, G. R. Smith, A. J. Tebben, *Synth. Commun.* **1995**, *25*, 3255; b) F. Lin, H.-Y. Peng, J.-X. Chen, D. T. W. Chik, Z. Cai, K. M. C. Wong, V. W.-W. Yam, H. N. C. Wong, *J. Am. Chem. Soc.* **2010**, *132*, 16383; c) S. Wiegmann, B. Neumann, H.-G. Stammler, J. Mattay, *Eur. J. Inorg. Chem.* **2012**, 3955.

Research Article
doi.org/10.1002/ejic.202300284

[14] P. Anbarasan, T. Schareina, M. Beller, *Chem. Soc. Rev.* **2011**, *40*, 5049.
[15] a) K. Sonogashira, Y. Tohda, N. Hagihara, *Tetrahedron Lett.* **1975**, *50*, 4467; b) S. Takahashi, Y. Kuroyama, K. Sonogashira, N. Hagihara, *Synthesis*, **1980**, 627.
[16] a) C. N. R. Rao, *Ultra-Violet and Visible Spectroscopy*, Butterworths, London **1961**, p. 39; b) T. Brotin, N. Vanthuyne, D. Cavagnat, L. Ducasse, T. Buffeteau, *J. Org. Chem.* **2014**, *79*, 6028.
[17] a) A. Collet, G. Gottarelli, *J. Am. Chem. Soc.* **1981**, *103*, 204; b) A. Collet, G. Gottarelli, *Croat. Chem. Acta* **1989**, *62*, 279.
[18] L. Erieu-Peyrard, C. Coiffier, P. Bordat, D. Bégué, S. Chierici, S. Pinet, I. Gosse, I. Baraille, R. Brown, *Phys. Chem. Chem. Phys.* **2015**, *17*, 4168.
[19] K. Sonogashira, Y. Fujikura, T. Yatake, N. Toyoshima, S. Takahashi, N. Hagihara, *J. Organomet. Chem.* **1978**, *145*, 101.
[20] a) G. Fuhrmann, T. Debaerdemaeker, P. Bäuerle, *Chem. Commun.* **2003**, 948; b) Z. M. Hudson, C. Sun, K. J. Harris, B. E. G. Lucier, R. W. Schurko, S. Wang, *Inorg. Chem.* **2011**, *50*, 3447; c) C. Y.-S. Chung, S. P.-Y. Li, M.-W. Louie, K. K.-W. Lo, V. W.-W. Yam, *Chem. Sci.* **2013**, *4*, 2453; d) R. Inoue, R. Kondo, Y. Morisaki, *Chem. Commun.* **2020**, *56*, 15438.
[21] a) S. Yamazaki, A. J. Deeming, *J. Chem. Soc. Dalton Trans.* **1993**, 3051; b) C. J. Adams, N. Fey, Z. A. Harrison, I. V. Sazanovich, M. Towrie, J. A. Weinstein, *Inorg. Chem.* **2008**, *47*, 8242; c) D. Fortin, S. Clément, K. Gagnon, J.-F. Bérubé, M. P. Stewart, W. E. Geiger, P. D. Harvey, *Inorg. Chem.* **2009**, *48*, 446.
[22] a) J. Fornés, E. Lalinde, A. Martín, M. T. Moreno, *J. Organomet. Chem.* **1995**, *490*, 179; b) M. D. Janssen, K. Köhler, M. Herres, A. Dedieu, W. J. J. Smeets, A. L. Spek, D. M. Grove, H. Lang, G. van Koten, *J. Am. Chem. Soc.* **1996**, *118*, 4817; c) H. Lang, K. Köhler, G. Rheinwald, L. Zsolnai, M. Büchner, A. Driess, G. Huttner, J. Strähle, *Organometallics* **1999**, *18*, 598; d) C. J. Adams, P. R. Raithby, *J. Organomet. Chem.* **1999**, *578*, 178; e) W.-Y. Wong, G.-L. Lu, K.-H. Choi, *J. Organomet. Chem.* **2002**, *659*, 107; f) W.-Y. Wong, G.-L. Lu, K.-H. Choi, *J. Organomet. Chem.* **2003**, *670*, 45.
[23] S. Sander, E. J. Cosgrove, R. Müller, M. Kaupp, T. Braun, *Chem. Eur. J.* **2023**, *29*, e202202768.
[24] a) C. W. Chen, H. W. Whitlock, Jr. *J. Am. Chem. Soc.* **1978**, *100*, 4921; b) S. C. Zimmerman, *Beilstein J. Org. Chem.* **2016**, *12*, 125.
[25] a) J. Leblond, A. Petitjean, *ChemPhysChem* **2011**, *12*, 1043; b) L. Benda, B. Doistau, B. Hasenknopf, G. Vives, *Molecules* **2018**, *23*, 990.
[26] In this section we use the notation (+)-[Pt(dppp)(**2**)$_2$] rather than [Pt(dppp)((+)-**2**)$_2$], etc. because we do not know the sign of the rotatory power of the CTB **2** that is incorporated in (+)-[Pt(dppp)(**2**)$_2$], etc..
[27] a) H. Zimmermann, P. Tolstoy, H.-H. Limbach, R. Poupko, Z. Luz, *J. Phys. Chem. B* **2004**, *108*, 18772; b) O. Lafon, P. Lesot, H. Zimmermann, R. Poupko, Z. Luz, *J. Phys. Chem. B* **2007**, *111*, 9453.
[28] S. T. Mough, J. C. Goeltz, K. T. Holman, *Angew. Chem. Int. Ed.* **2004**, *43*, 5631.
[29] T. G. Appleton, M. A. Bennett, I. B. Tomkins, *J. Chem. Soc. D* **1976**, 439.
[30] P. J. Stang, D. H. Cao, S. Saito, A. M. Arif, *J. Am. Chem. Soc.* **1995**, *117*, 6273.
[31] G. W. Parshall, *Inorg. Synth.* **1970**, *12*, 27.
[32] Gaussian 09, M. J. Frisch, G. W. Trucks, H. B. Schlegel, G. E. Scuseria, M. A. Robb, J. R. Cheeseman, G. Scalmani, V. Barone, B. Mennucci, G. A. Petersson, H. Nakatsuji, M. Caricato, X. Li, H. P. Hratchian, A. F. Izmaylov, J. Bloino, G. Zheng, J. L. Sonnenberg, M. Hada, M. Ehara, K. Toyota, R. Fukuda, J. Hasegawa, M. Ishida, T. Nakajima, Y. Honda, O. Kitao, H. Nakai, T. Vreven, J. A. Montgomery, Jr., J. E. Peralta, F. Ogliaro, M. Bearpark, J. J. Heyd, E. Brothers, K. N. Kudin, V. N. Staroverov, R. Kobayashi, J. Normand, K. Raghavachari, A. Rendell, J. C. Burant, S. S. Iyengar, J. Tomasi, M. Cossi, N. Rega, J. M. Millam, M. Klene, J. E. Knox, J. B. Cross, V. Bakken, C. Adamo, J. Jaramillo, R. Gomperts, R. E. Stratmann, O. Yazyev, A. J. Austin, R. Cammi, C. Pomelli, J. W. Ochterski, R. L. Martin, K. Morokuma, V. G. Zakrzewski, G. A. Voth, P. Salvador, J. J. Dannenberg, S. Dapprich, A. D. Daniels, Ö. Farkas, J. B. Foresman, J. V. Ortiz, J. Cioslowski, D. J. Fox, Gaussian, Inc., Wallingford CT, **2009**.

Manuscript received: May 15, 2023
Revised manuscript received: June 20, 2023